Department of Physics, Chemistry and Biology

Master's Thesis

Growth of Carbon Nanomaterials on SiC

Fang-Wei Chen

2014-08-11

LITH-A-IFM-EX--14/2961--SE

Linköping University Department of Physics, Chemistry and Biology
581 83 Linköping

Department of Physics, Chemistry and Biology

Growth of Carbon Nanomaterials on SiC

Fang-Wei Chen

Thesis work done at IFM

2014-08-11

Supervisor
Mikael Syväjärvi

Examiner
Valdas Jokubavicius

Linköping University
INSTITUTE OF TECHNOLOGY

Linköping University Department of Physics, Chemistry and Biology
581 83 Linköping

Avdelning, institution
Division, Department

Material Physics
Department of Physics, Chemistry and Biology
Linköping University

Datum
Date
2014-08-11

Språk
Language

☐ Svenska/Swedish
☒ Engelska/English

☐ _____

Rapporttyp
Report category

☐ Licentiatavhandling
☒ Examensarbete
☐ C-uppsats
☐ D-uppsats
☐ Övrig rapport

☐ _____

ISBN

ISRN: LITH-A-IFM-EX--14/2961--SE

Serietitel och serienummer **ISSN**
Title of series, numbering _____

URL för elektronisk version
http://www.ep.liu.se

Titel
Title

Growth of Carbon Nanomaterials on SiC

Författare
Author

Fang-Wei Chen

Sammanfattning
Abstract

Silicon carbide, a semiconducting material with properties competitive with silicon, has been under research to enhance performances of electronic devices recently. Carbon allotropes have also been noticeable nowadays for their great diversity in properties and geometries. The aim is hence to reproduce high quality bulk 3C-SiC by cubic sublimation growth process, observe thermal decomposition of silicon carbide and find the temperatures when the surface morphology changes, and have first trial of thermally driven attachment of carbon structures using nano-sized powder of carbon allotropes.

The cubic sublimation growth process had the silicon face of 4 degrees off-axis 4H-SiC substrates grown at 1850 ℃, 1900 ℃ and 1950 ℃ in vacuum, and characterized by optical microscopy. The thermal decomposition of silicon carbide had both silicon and carbon face of 4H-SiC on-axis substrates processed at 1600 ℃, 1700 ℃ and 1800 ℃ for five minutes, with 800 mbar of argon introduced once reaching 1000 ℃, and characterized by optical microscopy and atomic force microscopy. The thermally driven attachment of carbon structures had silicon face of 4H-SiC on-axis substrates distributed with powders of multi walled carbon nanotube, fullerene, diamond and graphene, and 3C-SiC as-grown substrates distributed with powder of multi walled carbon nanotube, and then processed at 1600 ℃, 1700 ℃ and 1800 ℃ for five minutes, with 800 mbar of argon introduced once reaching 1000 ℃, and characterized by optical microscopy and scanning electron microscopy.

The highest quality of bulk 3C-SiC, judged by its appearance under optical microscope, had been reproduced by cubic sublimation growth process at 1950 ℃, which is the highest growth temperature studied in this thesis. Thermal decomposition of silicon carbide had been seen in all samples with surface morphology modification under optical microscope and strain stripes under atomic force microscope, giving the opportunities of carbon structures attachment at all temperatures. Generally, the trend of thermally driven attachment of carbon structures samples followed a thermodynamic behavior. When islands successfully grew on the sample surface, larger island sizes existed at higher temperature since atoms had greater energy. In addition, multi walled carbon nanotubes grown on 3C-SiC substrates have smaller average islands size than on 4H-SiC on-axis substrates for the different conditions of roughness and polytypes of the substrates.

Nyckelord
Keyword

Silicon carbide, cubic sublimation growth process, thermally driven attachment of carbon structures, carbon allotropes

ABSTRACT

Silicon carbide, a semiconducting material with properties competitive with silicon, has been under research to enhance performances of electronic devices recently. Carbon allotropes have also been noticeable nowadays for their great diversity in properties and geometries. The aim is hence to reproduce high quality bulk 3C-SiC by cubic sublimation growth process, observe thermal decomposition of silicon carbide and find the temperatures when the surface morphology changes, and have first trial of thermally driven attachment of carbon structures using nano-sized powder of carbon allotropes.

The cubic sublimation growth process had the silicon face of 4 degrees off-axis 4H-SiC substrates grown at 1850 ℃, 1900 ℃ and 1950 ℃ in vacuum, and characterized by optical microscopy. The thermal decomposition of silicon carbide had both silicon and carbon face of 4H-SiC on-axis substrates processed at 1600 ℃, 1700 ℃ and 1800 ℃ for five minutes, with 800 mbar of argon introduced once reaching 1000 ℃, and characterized by optical microscopy and atomic force microscopy. The thermally driven attachment of carbon structures had silicon face of 4H-SiC on-axis substrates distributed with powders of multi walled carbon nanotube, fullerene, diamond and graphene, and 3C-SiC as-grown substrates distributed with powder of multi walled carbon nanotube, and then processed at 1600 ℃, 1700 ℃ and 1800 ℃ for five minutes, with 800 mbar of argon introduced once reaching 1000 ℃, and characterized by optical microscopy and scanning electron microscopy.

The highest quality of bulk 3C-SiC, judged by its appearance under optical microscope, had been reproduced by cubic sublimation growth process at 1950 ℃, which is the highest growth temperature studied in this thesis. Thermal decomposition of silicon carbide had been seen in all samples with surface morphology modification under optical microscope and strain stripes under atomic force microscope, giving the opportunities of carbon structures attachment at all temperatures. Generally, the trend of thermally driven attachment of carbon structures samples followed a thermodynamic behavior. When islands successfully grew on the sample surface, larger island sizes existed at higher temperature since atoms had greater energy. In addition, multi walled carbon nanotubes grown on 3C-SiC substrates have smaller average islands size than on 4H-SiC on-axis substrates for the different conditions of roughness and polytypes of the substrates.

ACKNOWLEDGEMENTS

Before the main content of my thesis, I would like to show my gratitude to the people who helped me with this thesis work in all ways. It would not be possible for me to accomplish my master thesis without all the helps, and I indeed appreciate them.

- **Mikael Syväjärvi**, my examiner, for having me in the group doing my diploma thesis work, planning the experimental details and discussing the results together, and giving all the comments on the thesis.

- **Valdas Jokubavicius**, my supervisor, for demonstrating and teaching me the knowledge required in the lab, helping me with the characterizations of the samples, and also giving the suggestions.

- The people that had given me technical helps and valuable comments; especially **Reza Yazdi** for the help in AFM measurements, and **Philipp Schuh** for the help and cooperation in the growth series.

- My family and friends that have been there for me all the time; especially **Victor Johansson** for being supportive in my life, and **Keng-Yu Lin** for being my friend and opponent here.

CONTENTS

1. INTRODUCTION

Silicon carbide (SiC) is a semiconducting material with properties such as wide bandgap, high thermal conductivity, high saturated electron drift velocity and high electric field breakdown strength. The material has capability to operate at high temperature, high power and high frequency, and it is radiation-resistant in addition. Combining the properties and possibilities with its commercial availability of substrates, silicon carbide has been under research to enhance performances of electronic devices, which are mostly based on silicon nowadays [1].

Silicon carbide therefore is a good base material for further studies, especially since it is a semiconductor material. Among the polytypes, 4H and 6H-SiC are the most common ones and are the only ones which are commercially available so far. In comparison, the 3C-SiC has a number of benefits, while the growth is more challenging.

Carbon allotropes have a great diversity. Fullerenes (a spherical form of carbon atoms) and carbon nanotubes (cylindrical form of carbon atoms) have a long history, while recently graphene has emerged as a two dimensional (planar) form of carbon atoms. The various allotropes have different properties and geometries, and therefore the combination of SiC with different allotropes on its surface could give rise to a new platform of possibilities for new devices.

In this work we have explored a novel approach of growth of 3C-SiC that gives high quality material. And in the end, we demonstrate the combination of carbon allotropes with 3C-SiC as substrate.

The 6H and 4H-SiC polytypes have been explored extensively. On the other hand, there are some properties that make 3C-SiC very interesting and worthwhile to study. In metal on semiconductor structures, 4H-SiC have faced challenges with interface states in the bandgap which cause a low electron mobility. The lower bandgap makes these states to be in conduction band in 3C-SiC, and should therefore cause less problems regarding influence on the electron mobility. Also, the hole mobility in 4H-SiC is low, while in 3C-SiC both the electron and hole mobilities are high. This, for example, is interesting for applying 3C-SiC as water splitting device [2]. In such, the surface activity is important, and a 3C-SiC that is modified with a geometrical surface layer could be beneficial in order to handle both electrochemistry and electron transfer from the semiconductor to the solution. Further on, there is an emerging research in biofuel cells that convert waste water to energy, where the active electrodes are important. The chemical resistivity of SiC in electrochemistry makes it suitable for the research while a carbon electrode material could be applied for the surface activity. The 3C-SiC which is doped with boron is very suitable for the intermediate bandgap solar cell [3]. In this approach, an intermediate band in the bandgap creates three energy levels which could collect three parts of the solar spectrum within one semiconductor. Thereby many issues with interface between different materials, that collect sun light in different parts, could be avoided. Finally, it was indicated that 3C-SiC could be a better suited material for growth of graphene [4]. Not only does this imply that the novel structures combining 3C-SiC and graphene could emerge, but graphene could also be very suitable as contact material on doped 3C-SiC for solar cell. Thereby the graphene could be a base material on SiC on which carbon allotropes are attached to make a modified surface structure for any activity in which the electrode properties and surface activity is important. Further on, the knowledge in carbon allotropes on SiC would open a new research field that can pave

the way for interesting scientific findings. The growth of carbon allotropes on SiC has never been studied, and this thesis work explores the first studies in this approach.

2. SILICON CARBIDE

2.1 POLYTYPES

The unit structure of SiC crystal is a tetrahedron of Si and C atoms, as shown in Figure 1 with strong bonds in between the atoms. As the bonded Si-C tetrahedrons stack up, the differences of the stacking sequences of the double layers along the c-axis in the hexagonal frame of reference give rise to the polytypes. The normal stacking orders of the two other directions, on the other hand, are identically close-packed. While there are almost infinite number of possible polytypes, approximately 200 polytypes have been discovered, the most common ones among them are 3C-SiC, 4H-SiC, 6H-SiC and 15R-SiC. The abbreviations H, C and R stand for hexagonal (H), cubic (C) and rhombohedral (R) crystal structures, while the numbers denote the number of double layers required for periodicity. In this thesis, 3C-SiC and 4H-SiC are studied, and hence will be introduced briefly below with Figure 2 and text.

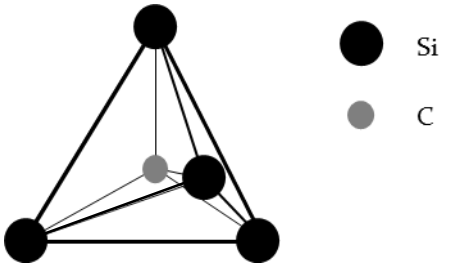

Figure 1: The tetrahedral structure of SiC unit.

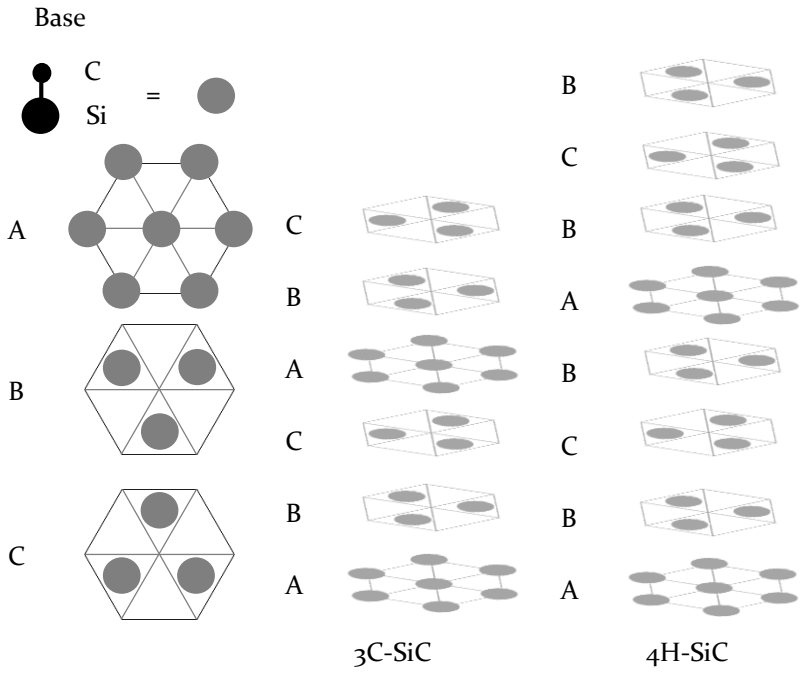

Figure 2: The stacking sequences of 3C-SiC and 4H-SiC.

3C-SiC

The 3C-SiC is the only one polytype of cubic SiC, also denoted β-SiC. The stacking sequence is ABCABC... in the <111> direction, where A, B and C are the layers with different positions with respect to the lattice. The crystallographic structure of this arrangement is purely cubic zinc blende, which is identical to Si and GaAs that are the commonly used semiconductor materials in electronics. Among the known polytypes, 3C-SiC has the smallest bandgap (~2.4 eV), and one of the largest electron mobility (~1000 $cm^2V^{-1}s^{-1}$ in low-doped material). Besides, it also has fascinating properties such as isotropic physical properties and biocompatibility. Despite the interesting properties it might possess, the different growth mechanism and difficulties in polytype stability control make it less studied and still unavailable as commercial substrate at the moment.

4H-SiC

The 4H-SiC is one of the hexagonal symmetry polytypes, hence belonging to the group of α-SiC. It consists of a mixture of same amount of zinc blende (cubic) and wurtzite (hexagonal) bonds. The stacking sequence is ABCBABCB... in the c-axis, where A, B and C are the layers with different positions with respect to the lattice. The 4H-SiC and 6H-SiC are currently the only SiC polytypes available in bulk wafer form [1] [5].

2.2 Properties

Since the polytypes of SiC only differ in the stacking sequences of the double layers along c-axis, the difference in the properties of the polytypes is not profound. Hence, the properties in the following paragraphs would be in general for SiC, while the minor differences between the polytypes could be broadening the application areas, as described in the introduction.

The SiC polytypes have wide bandgap, from 2.4 eV for 3C-SiC till 3.3 eV for 4H-SiC. This results in low leakage currents at high temperatures (>700 °C). They also have high current densities and extremely high thermal conductivity (5 W/cmK). In addition, the wide bandgaps and small lattice constants (4.36 Å for 3C-SiC; a= 3.08 Å and c= 10.08 Å for 4H-SiC) contribute to a high breakdown electric field (4 MV/cm). Due to these mentioned properties, SiC could be a promising high-power device material even avoiding the design of massive cooling system and reducing the consumption of power.

They also have high saturated electron velocity, ranging from 2.0×10^7 cm/s for 4H-SiC to 2.7×10^7 cm/s for 3C-SiC. Thereby, SiC would be capable of generating large power at high frequencies, and applied for the using of radars or as microwave source in many applications by replacing electronic tubes with the SiC devices.

In comparison with Si, the most commonly applied electronic material, the properties mentioned above of SiC are superior. For Si, the values are 1.1 eV for bandgap energy, 1.5 W/cmK for thermal conductivity, 5.43 Å for lattice constant, 0.3 MV/cm for breakdown electric field and 1.0×10^7 cm/s for saturated electron velocity. The SiC is therefore prospective for replacing Si in the high-power, high-temperature and high-frequency demanded devices in the future with better performances.

In addition, the high chemical stability of SiC enables the devices with SiC as substrates to be working in chemically aggressive environment. For instance, high chemical stability and high

temperature stability would be required for the sensors mounted close to the engines in the car industry [5] [6].

2.3 Mechanisms for 3C-SiC Nucleation and Growth

Though it had been known for decades that SiC has potential in superior performances, the material has not yet been widely developed and applied. This is due to the fact that quality and stability control of the polytypes are not yet well-known and in many cases still under research. The growth process of SiC is dependent on plenty of factors, while ones such as supersaturation level of the source, Si/C ratio and the species of the substrate are known. This is in particular the case for 3C-SiC and there is a lot of work needed to understand the growth. The two mechanisms for nucleation and growth of 3C-SiC are introduced in the paragraphs below, which are the step-flow and the two-dimensional nucleation (island) growth. These two mechanisms are both taking part and in fact competing in the real surface growth, while step-flow takes place prior to 2-D nucleation and island growth generally in this case, due to the 4 degrees off-axis of our 4H-SiC substrate. As the high activation energy and high supersaturation level reached, the growth is then dominated by 2-D nucleation and island growth. The mechanism for 4H-SiC growth is, however, not introduced here since we have used purchased 4H-SiC substrates which are commercially available.

Step-Flow

The step-flow growth often starts at the edge of a vicinal or stepped surface during growth. In this thesis, low (4 degrees) off-axis 4H-SiC substrate, which in our case results in approximately 200 nm for step width and 10 nm for step height, is applied. The step-flow growth is the main mechanism of the initiate stage of 3C-SiC enlargement. The growth of step-flow and expansion of 3C-SiC coverage is along the $< 11\bar{2}0 >$ direction of the 4H-SiC substrate.

The 3C-SiC nucleation process starts with the atoms subliming from the source that arrive on the surface of the substrate. These arriving atoms either adsorb and stay on the surface as adatoms or desorb and leave back to the ambient. For the adatoms that stay on the surface, they diffuse randomly along the surface and meet thermodynamically and energetically favored positions. These could be surface features such as steps, kinks, islands or defects, where they can nucleate. The nucleation sites would then be initiating the process and the nucleation and growth thus start. The illustration of the surface features and the adatoms is shown in Figure 3.

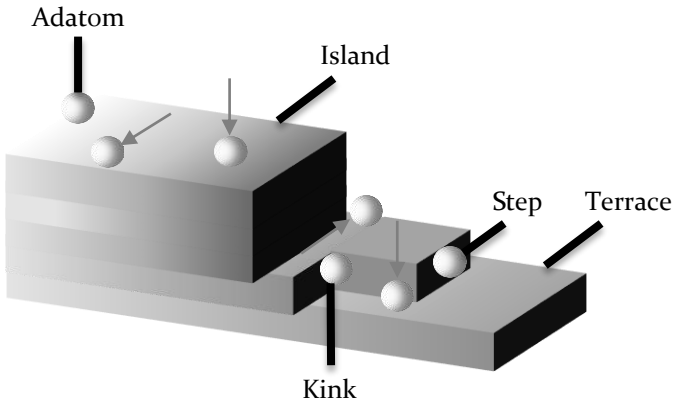

Figure 3: The illustration of surface features and adatoms.

Growth and expansion would continue at the nucleation sites with the incoming adatoms that are accumulating. The island growth stage is then followed by island coalescence and continuous film growth, forming a large terrace along the step-flow direction. Typically this occurs at the edge of the sample, and the 3C-SiC expands over the sample as the material continues to grow. At the very first stage before 3C-SiC formation, there is a homo-epitaxial growth of 4H-SiC layer on the 4H-SiC substrate. At the edge there is a basal plane that is formed, and the 3C-SiC can nucleate on the basal plane. Nevertheless, during the island coalescence, defects such as twin boundaries and stacking faults may be formed, so the amount of nucleation sites should be minimized and only a few large domains will then be formed in order to achieve good quality growth. The illustration of the formation of 3C-SiC terrace by step-flow growth is shown in Figure 4 [7] [8].

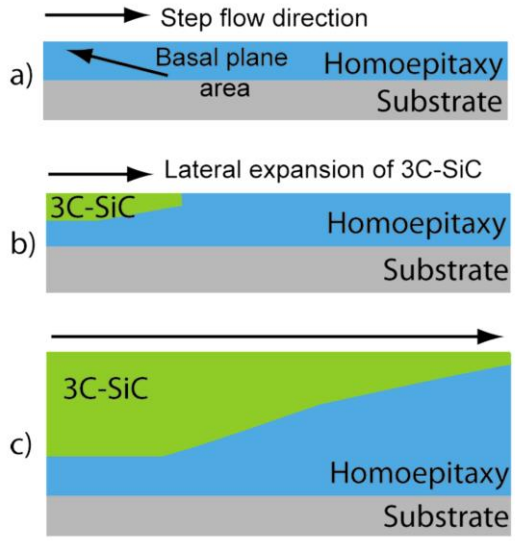

Figure 4: The formation of 3C-SiC terrace by step-flow growth [4].

Two-Dimensional Nucleation and Island Growth

The two-dimensional nucleation and island growth is the main mechanism for the 3C-SiC growth on on-axis substrates, and it is the mechanism for the subsequent 3C-SiC growth in our case after the initial homo-epitaxial growth on the low off-axis substrate. It takes place at a flat terrace area with low density of steps that is formed at the edge which would correspond to the large 3C-SiC terrace formed by initial homo-epitaxial step-flow growth.

High activation energy and high supersaturation level of the sublimed gas atoms are required for the two-dimensional nucleation to occur. This indicates that the mechanism favors the 3C-SiC formation, since high supersaturation ratio and high Si/C ratio has been favorable growth conditions for 3C-SiC to form on silicon carbide on-axis substrates. The supersaturation ratio refers to the supplied vapor pressure above the substrate and the equilibrium vapor pressure at the surface. The two-dimensional nucleation and island growth hence dominate the 3C-SiC growth under the controlled circumstances and expand laterally in coverage of the substrates and also vertically in thickness [9].

2.4 DEFECTS

The defects are one of the main problems restraining the development and application of SiC. Besides the thermodynamically existing defects from growth, the bulk production also causes ones that are difficult to avoid in reality. The major defects in SiC such as dislocations, micropipes, double positioning boundaries, stacking faults and step bunching are briefly mentioned in the following paragraphs.

DISLOCATIONS

Dislocations are line defects due to internal stress resulting from the lattice constant difference between the epilayer and the substrate, lattice domain misalignment or the external force applied on the lattice. In order to reduce and release the stress in the lattice, dislocations may be introduced by plastically shifting the atoms situated on the lattice points. The high density of dislocations has been a problem since it hinders the use of SiC in electronic devices, which is within $10^3 - 10^4 cm^{-2}$ in the best cases [10].

There are two types of them, which are edge dislocation and screw dislocation respectively as illustrated in Figure 5. A perfect crystal without dislocations could enclose a loop without introducing any Burgers vector in all lattice directions. On the other hand, Burgers vector that is perpendicular to dislocation line is required for lattice with edge dislocation to enclose the loop, and Burgers vector that is parallel to dislocation line is required for lattice with screw dislocation to enclose the loop. In the reality, edge and screw dislocations are often mixed in addition to the single cases.

MICROPIPES

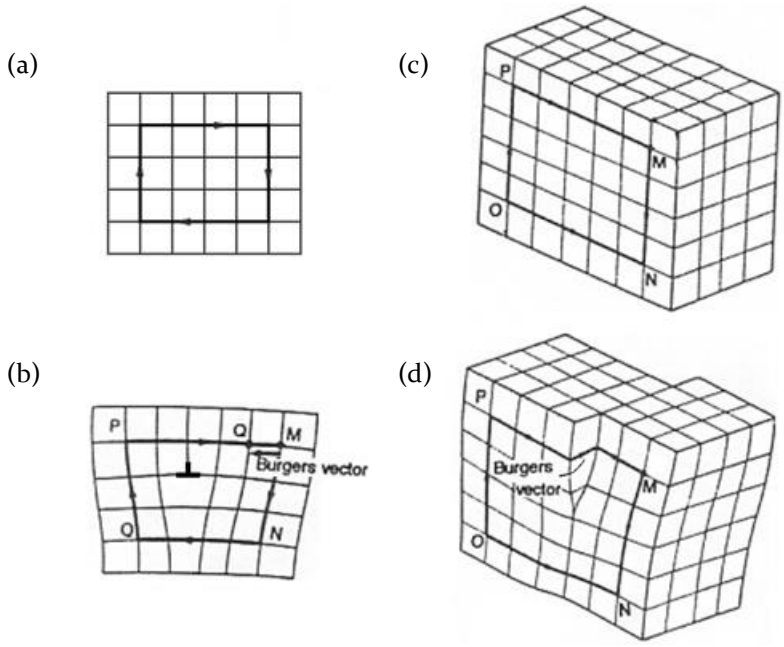

Figure 5: (a) the reference circuit for a perfect crystal (b) the Burgers vector of edge dislocation formed in the Burgers circuit (c) the reference circuit for a perfect crystal (d) the Burgers vector of screw dislocation formed in the Burgers circuit [12].

Micropipes are bulk defects (voids), also known as micropore, microtube, capillary or pinhole defects. The degradation of breakdown voltage in electronic devices made of SiC is often caused by them. Among the possible mechanisms for them to form, the most known and believed one suggests that they are open core superscrew dislocations that propagate along the c-axis from the substrate and may penetrate into the growing epilayer. Nonetheless, since the micropipes are formed from the screw dislocations with large Burgers vectors, according to the mechanism explained above, in the initiation stage of nucleation as the other defects, possibilities of dislocations and micropipes merging and annihilating could lead to lower densities of the defects in the later stages. Micropipes are known to disturb the step flow growth, and can cause polytype disturbances [10] [11] [12].

Stacking Faults

Stacking faults are planar defects given rise from the disordered stacking sequences. The low formation energy of stacking fault in SiC has been supported due to the fact that closest packing structure could be formed in crystal structure with stacking fault. Taking 3C-SiC for instance, the normal stacking sequence is ABCABC in the <111> direction. In the intrinsic stacking fault case, it could become ABCACABC with a plane B missing in this case; in the extrinsic stacking fault case, it could become ABCABACABC with an extra plane A in this case. Since stacking sequences are the differences in the polytypes of SiC, stacking faults could then alter the properties of the grown SiC and are hence of great importance [13].

Double Positioning Boundaries

Double positioning boundaries (DPBs) are one of the defects commonly discovered in 3C-SiC. The DPB is the boundary defined by having separating domains related by a 180° twin axis, nucleation occurring at the interface and relatively high energy. Combining the two equivalent stacking sequences, which are ABCABC and CBACBA, and the different orientations of domains, difficulties exist while different stacking sequences from domains attempt to merge during coalescence [14].

Step Bunching

Step bunching is a phenomenon occurs in step-flow growth material. Though the mechanism has not yet been systematically understood, there have been several models interpreting the phenomenon during the growth. According to the research from Schwoebel et al., the adatoms diffusing down a step possess an additional energy barrier than those leaping on a flat terrace. And from the research team of Kimoto et al., on the other hand, the step bunching is proposed as a surface equilibrium process that minimizes the free energy during the growth. Hence, the microsteps catch up and superimpose with others due to their different lateral growth speeds and form macrosteps whose heights are several nanometers, or even up to 100-1000 nm. The accumulated macrosteps could then lead to micrometer-sized defects in the continual growth and give rise to rough surface and degradation of crystal quality [12].

3. ALLOTROPES OF CARBON

Carbon has been a topic of great research interest in a long period of time for numerous reasons, such as being an abundant element in the universe and the second-most common element in human body, having capability of bonding with other elements and further forming stable species, and existing in a number of allotropes. In addition, it has been applied in this thesis for its possibility of forming carbon-carbon or silicon-carbon bonds between SiC substrate and carbon nano-sized powder, providing combinations for future research basis and potential uses.

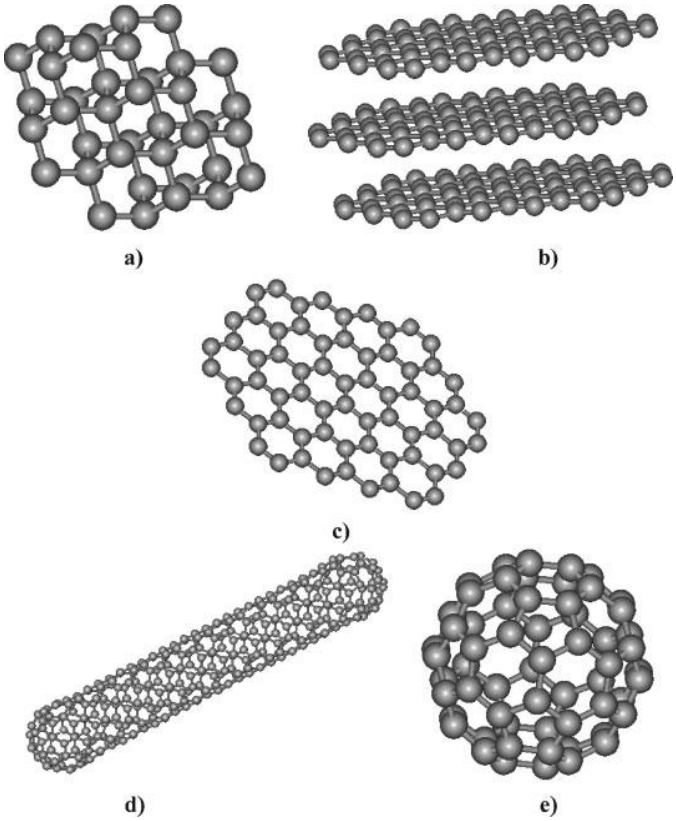

Figure 6: The common allotropes of carbon: (a) diamond (b) graphite (c) graphene (d) single wall carbon nanotube (e) Buckminsterfullerene [16].

Allotropes of carbon are the various crystalline structures in which carbon could exist. Classified by dimensions, the most common ones are three-dimensional diamond and graphite, two-dimensional graphene, one-dimensional carbon nanotube (CNT) and zero-dimensional Buckminsterfullerene, as shown above in Figure 6. Nano-sized powder of diamond, graphene, multi walled carbon nanotubes (MWCNT) and fullerene have been of our interest and hence selected for the attaching trials in this thesis work.

DIAMOND

Diamond is built of carbon atoms in tetrahedral orientation. It is known to be one of the hardest material and also a good thermal conducting material. On the other hand, it is brittle and has poor electrical conductivity. With further research, diamond could be an excellent semiconductor [15].

GRAPHENE

Graphene is a relatively newly discovered allotrope of carbon. It is a single sheet of carbon atoms with similar structure to graphite. Graphene has high electrical conductivity (for the delocalized electrons throughout the material) and high thermal conductivity. It is also one of the strongest materials [15].

CARBON NANOTUBE

Carbon nanotubes (CNTs) are also a fascinating discovery as allotrope of carbon, made of graphene sheet rolled into tubular structure and could have half-fullerene capped at both ends. Carbon nanotubes have both single walled carbon nanotubes (SWCNTs) and multi walled carbon nanotubes (MWCNTs) structures. They have light mass, high tensile strength, thermal conductivity and magnetic reluctance, and their properties are depended on their structural properties [15].

FULLERENE

Fullerenes are carbon structures based on 12 pentagonal faces and any number of hexagonal faces with unlimited of combinations. The first observed and most famous one is C_{60}, consisting of 20 hexagons and 12 pentagons. They have poor conductivities since the molecules are held to each other by only weak Van der Waal's force [15].

4. Growth Techniques

4.1 Cubic Sublimation Growth Process

Most growth processes originate from the modified Lely process and are based on the physical vapor transport (PVT) principle. The cubic sublimation growth process (CSGP) has been studied for some years and is also applied in this thesis for 3C-SiC growth. The mechanisms for nucleation and growth have been mentioned in previous sections, the actual setup of the growth process in this thesis is mainly composed of heating system with Radio Frequency (RF) generator and vacuum system with turbo pump. The growth container is placed inside a quartz tube that is being pumped by the system.

As many parts are involved in both systems, the heating system is more relevant to the growth control. The system is illustrated below in Figure 7. The copper coils surrounding the quartz tube generate heating of the crucible when the current is passing through the coils and magnetic fields are induced. The cylindrical graphite crucible in the quartz tube is thus being heated up to provide temperature distributions for growth. The crucible is surrounded by a thermal insulation that is made of porous graphite foam which encloses the crucible system and does not couple with the magnetic field. The temperature is measured on top of the crucible and maintained in the range of 1850-1950 ℃ during the growth process for 3C-SiC in this thesis. Nevertheless, temperature gradients still exist. This is on one hand desired, since temperature gradient between the source and substrate is needed for the sublimation process to take place, but on the other hand not favored since the actual growth temperature determination would be difficult when it is only detected by the pyrometer at the top part of the crucible through the small hole of the insulating foam.

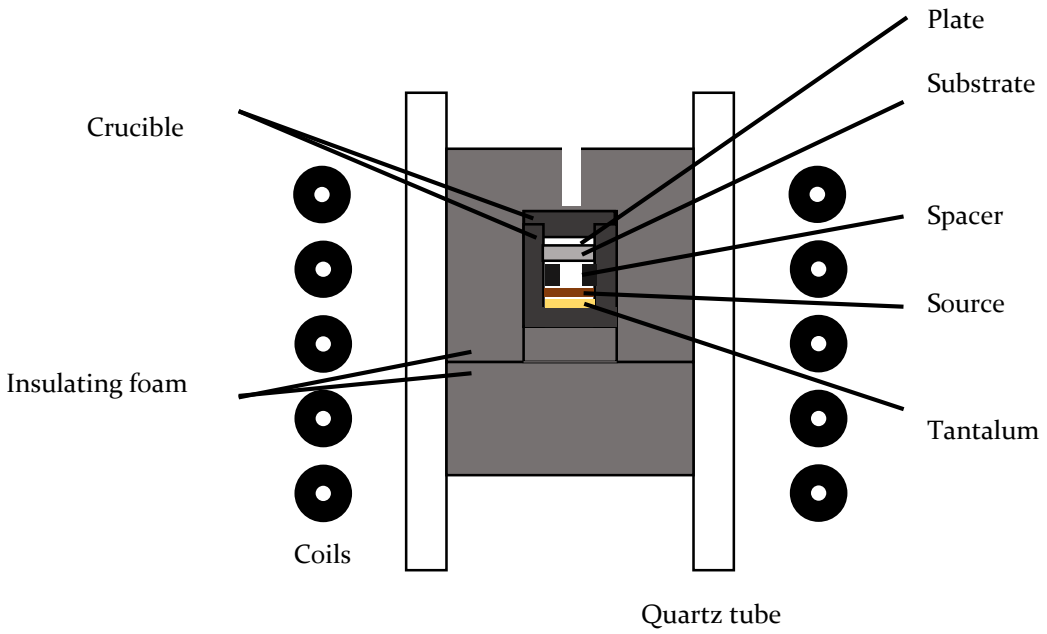

Figure 7: The illustration of the CSGP heating system and the inner structure of the crucible.

The inner setup of the crucible has been built to fit a growth structure according to the sandwich method with a source and a substrate separated by a graphite plate that acts as a spacer. Epitaxial growth of 3C-SiC on 4 degrees off-axis 4H-SiC substrate occurs inside the chamber with the setup design and environment control. The temperature gradient favors the sublimation of the source to take place, and the polycrystalline SiC source material with higher temperature sublimes to form vapor species that are deposited on the 4H-SiC substrate with lower temperature. A graphite spacer with a hole in the center is placed in between source (at bottom of crucible) and substrate (on top with surface facing downwards to source). The separation is 1 mm so that the sublimed gas can have a direct mass transport from source to substrate and are not reacting with the crucible wall. In addition, a graphite plate has been placed on top of the structure (backside of substrate) for preventing backside sublimation. At the bottom of the crucible, a tantalum foil is placed to serve for multiple purposes. The Si/C ratio and hence the polytype of SiC grown can be controlled by forming TaC; the graphitization inside the chamber is then reduced; the formation of voids, dislocations, second-phase inclusions and other structural and morphological defects is decreased. Since a fresh Ta foil is needed to getter carbon, used tantalum foils is needed to be replaced by new ones since the formation of TaC requires abundant of tantalum to react [16] [7].

The quartz tube is being pumped prior to the growth process till vacuum level, which is as far as 10^{-5} $mbar$ using the turbo pump. The reduction of impurities further supports the quality of grown 3C-SiC. The decrease of ambient pressure improves the speed of sublimation and hence the growth.

4.2 Thermal Decomposition of SiC

Since the 4H-SiC on-axis substrates used in this thesis work have been polished at the Si-rich face by the supplying company, the roughness required for the carbon structures to attach on is not enough. In order to have thermally driven attachment of carbon structures on the SiC substrates, the surface morphology of the substrates has to be modified into microscopically rough surface.

Therefore, thermal decomposition of SiC has been tested and observed as the pretreatment of thermally driven attachment of carbon structures. According to different temperatures and hence the thermal energy, the tendency of surface decomposition and atoms subliming should also differ. Nevertheless, once the temperature of heating has reached 1000 °C, 800 mbar gas flow of Ar is introduced into the chamber for suppressing the speed of sublimation. For comparison of the surface modification and the attaching effect from the thermal decomposition, it has been carried out at different temperatures.

4.3 Thermally Driven Attachment of Carbon Structures

Thermally driven attachment of carbon structures on SiC substrates have been carried out in this thesis work. The exact mechanism for thermally driven attachment of carbon structures is not known, but temperature is certainly one of the key factors. For attaching the nano-sized powder of different carbon allotropes to SiC surfaces, the experiments are at elevated and different temperatures for having initial surface modification and possibly a thermal decomposition of SiC and attachment of carbon. From observing the temperature effect of the thermally driven attachment, we may initiate an understanding about process which has not been studied previously.

As illustrated below in Figure 8, the arrangement is similar to the one of CSGP, with the same quartz tube, RF coils, RF generator and vacuum system. A SiC substrate is placed on two graphite bars serving as support. Carbon nano-sized powder is then evenly distributed onto the surface of substrate. Crucible and insulating foam are then closed, and placed into quartz tube for heating. Once the temperature of heating has reached 1000 ℃, 800 mbar gas flow of Ar is introduced into the chamber for suppressing the speed of sublimation as in thermal decomposition of SiC. The crucible has also been modified for having more even distribution of heat by a redesigned insulating foam and crucible.

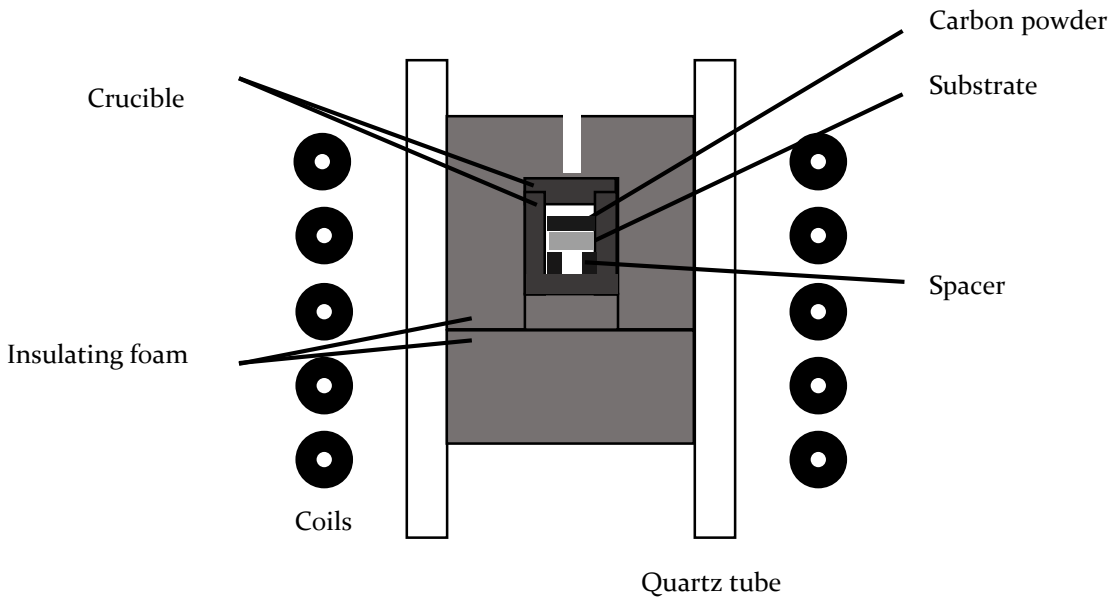

Figure 8: The illustration of the thermally driven attachment of carbon structure system and the inner structure of the crucible.

5. Characterization Techniques

For understanding the control of growths, ensuring the quality of samples and accuracy of results, characterizations for samples at each stage are necessary. In this thesis, Nomarski microscopy, scanning electron microscopy and atomic force microscopy are utilized as characterization techniques.

5.1 Nomarski Microscopy

The Nomarski microscopy is an examination mode based on optical microscopy which gives overview inspections of sample surface morphology, but with the capability of distinguishing finer height difference than conventional optical microscopy due to diffraction interference contrast (DIC). The optical arrangement of the microscopy in reflected light mode, which has been utilized in this thesis work for nontransparent carbon allotropes layers and so on, is sketched in Figure 9. The incident light beam firstly passes through polarizer and $\frac{\lambda}{2}$-plate, generating polarized light beam. The beam is then split into two parallel beams by double quartz prism, also known as DIC prism, and continue to travel in slightly displaced angles. When the beams arrive at the specimen, reflection occurs and the beams pass through DIC prism again and recombine. According to the morphology of the specimen surface, different optical paths take place and interference effects occur as a result. The advantage of finer height difference distinction is accomplished due to the interference pattern. On the other hand, the transmission light mode can be applied for transparent specimen such as yellowish 3C-SiC as-grown layer in this thesis work. The setup is similar to the reflection light mode, except there are two DIC prisms respectively splitting the incident beam and recombining the reflected beams [17].

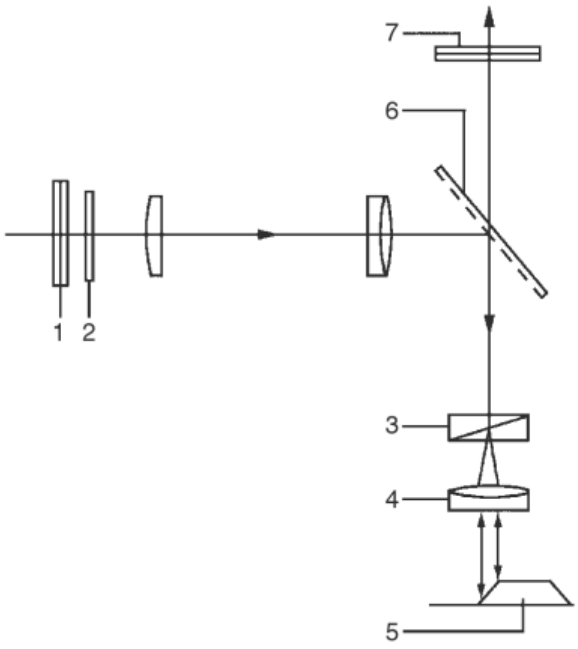

Figure 9: The optical arrangement of Nomarski microscopy in reflected light mode. 1- polarizer; 2- λ/2-plate; 3- DIC prism; 4- objective lens; 5- specimen; 6- light reflector; and 7- analyzer [13].

5.2 Scanning Electron Microscopy

The scanning electron microscopy (SEM) has been applied in this thesis for investigating the surface topography at higher magnification, better depth of focus, three dimensional appearance and it gives a fast feedback since it needs only a fairly simple sample preparation.

The electron beam is focused and directed by electromagnetic fields to the sample. The narrow beam, which limits the resolving power, is then scanning on the surface of sample. While the electron

beam is interacting with the sample, different signals such as secondary electrons, back scattering electrons, Auger electrons and characteristic X-rays are created. By amplifying and processing the signal created, images of sample topography with high resolution are obtained [18].

5.3 Atomic Force Microscopy

The atomic force microscopy (AFM) has been utilized in this thesis for its capability of resolving 3D images of sample surface morphology at an atomic level, i.e. at Ångström level, while the sample pre-treatment is fairly simple and the process is non-destructive. Besides the general surface morphology mapping, detailed and numerical information of samples can be given by using this technique.

Originated from scanning tunneling microscopy (STM), atomic force microscopy has been invented for expanding the application to not only metals and semiconductors which are conductive but also insulating surfaces. The principle of AFM is the same as STM, while not based on the tunneling current that is decreasing exponentially with increasing tip-sample distance, but the Van der Waals force of atoms between the tip and sample. Since the interacting force is between surface atoms from tip and sample, the surface morphology in atomic resolution is resolved. Nevertheless, this also results to a rather low scanning speed and small scanning area. The limiting factors are the tip sharpness and the detector resolving power.

Among the three modes which have been developed for AFM so far, which are contact mode, non-contact mode and tapping mode, the tapping mode has been chosen for characterizing the samples in this thesis work. Due to the vibration of cantilever and thereby tip during scanning of tapping mode, short tip-sample distance and fine resolution should be used while also minimizing surface modification of sample and mechanically damage of both tip and sample. When the tip is brought towards the sample surface, the Van der Waals force between the tip and sample can lead to a cantilever deflection according to Hooke's law. The deflection is measured with a reflected laser beam from the top of cantilever detected by the photodiodes, and the cantilever shall be adjusted from feedback signals. From the z axis information acquired scanning in x-y axis line by line and interpreted by processor, the 3D images of the sample surface are constructed [6].

6. Experimental Details

The experimental details such as descriptions of each process, parameters during the experiments and information of samples are given in this chapter. In addition, a procedure of outgassing is carried out in between each sample series. Outgassing should remove the possible contamination in the chamber by heating up the system in vacuum till 2000 ℃ that is kept for 15 minutes. A reference run is between growth series to ensure that the conditions of growth remain the same.

6.1 Cubic Sublimation Growth Process

Having the 4 degrees off-axis 4H-SiC substrate loaded in the system as described previously for CSGP, the quartz tube is pumped overnight prior to the growth process to ensure the vacuum level, which is about 10^{-5} $mbar$ with the use of the turbo pump. Then with the cooling water running, the RF generator is turned on and tuned according to the recipe from a run card that is used to document the experiment. The ramp up of heating rate is approximately 20 K/min until the desired growth temperature. Then the growth temperature is maintained until the growth time for desired thickness of sample is reached. The cooling down process is then followed, with the RF generator is off for at least two hours, until crucible is at room temperature. Argon is then introduced to 980 mbar, and the sample can be loaded out. In addition, the source used in the 3C-SiC growth is from Mitsui Engineering Company. The sample information is shown below in Table 1.

Table 1: The sample series list of 3C-SiC grown by CSGP on 4 degrees off-axis 4H-SiC substrates at different temperatures.

	T (℃)	t (min)	Thickness (μm)	Growth rate (μm/h)
ELS537	1850	210	874	250
ELS539	1900	105	975	557
ELS542	1950	50	850	1020

6.2 Thermal Decomposition of SiC

Having the 4H-SiC on-axis substrate in the setup as described previously for thermal decomposition of SiC, the quartz tube is pumped overnight prior to the thermal process to ensure the vacuum level, which is about 10^{-5} $mbar$ with the use of the turbo pump. Then with the cooling water running, the RF generator is turned on and tuned according to the recipe from run cards. The ramp up of the heating rate is approximately 20 K/min until the desired temperature has been reached. In the duration of heating, once the temperature has reached 1000 ℃, 800 mbar gas flow of Ar is introduced into the chamber. When the desired temperature is reached, it is kept for 5 minutes. The cooling down process is then taken place with the RF generator off for at least two hours until Ar is introduced to 980 mbar so that the sample can be unloaded. The sample information is shown as below in Table 2.

Table 2: The sample list of thermal decomposition of SiC performed on 4H-SiC on-axis substrate at different temperatures and different sides of substrates.

	S601	**S602**	**S603**	**S604**	**S605**	**S606**
Side up	C	Si	C	Si	C	Si
T (℃)	1800		1700		1600	

6.3 Thermally Driven Attachment of Carbon Structures

Prior to loading substrate and powder, the quartz tube is pumped overnight prior to the growth process to ensure a good vacuum level ($10^{-5}\ mbar$). After the pumping, the vacuum system is turned off and the Ar is introduced until atmospheric pressure is reached so that the insulator and the crucible can be taken out from the quartz tube. The 4H-SiC on-axis or 3C-SiC substrate is then placed in the crucible with nano-sized carbon powder distributed on the surface, and the insulator and crucible are loaded in the system again. Then with the cooling water running, the RF generator is turned on and tuned according to the recipe from run cards. The ramp up of the heating rate is approximately 20 K/min until the temperature has reached 1000 ℃, at which 800 mbar of Ar is introduced into the chamber, at a continued temperature ramp up. When the desired process temperature is reached, it is maintained for 5 minutes. The cooling down process is then followed until the sample can be unloaded. In addition, the samples of thermally driven attachment of carbon structures had been blown using a nitrogen gun blow to remove any residual unattached powder on the surface. Thus the carbon structures that are observed are likely to be attached. The sample information is shown as below in Table 3 and Table 4. Nevertheless, the 3C-SiC samples (ranging from ELS533 till ELS545 at 1950 ℃ growth temperature) were grown at similar conditions like described in the 3C-SiC samples described in the growth section.

Table 3: The sample list of thermally driven attachment of carbon structures with MWCNTs, fullerene, diamond, graphene and reference run with only bare substrate performed on 4H-SiC on-axis substrates at different temperatures.

	st01	**st02**	**st03**	**sf01**	**sf02**	**sf03**	**sd01**	**sd02**	**sd03**	**sg01**	**sg02**	**sg03**	**s000**
Substrate	4H-SiC on-axis												
Polytype	MWCNTs			fullerene			diamond			MWCNTs			-
T (℃)	1800	1700	1600	1800	1700	1600	1800	1700	1600	1800	1700	1600	1600

Table 4: The sample list of thermally driven attachment of carbon structures with MWCNTs performed on 3C-SiC substrates at different temperatures.

	ELS525	**ELS522**	**ELS526**
Substrate	3C-SiC		
Polytype	MWCNTs		
T (℃)	1800	1700	1600

7. Results and Discussions

This chapter includes the results, interpretations and discussions of this thesis work. The samples from CSGP have been characterized by optical microscopy; the samples from thermal decomposition of SiC have been characterized by Nomarski microscopy and atomic force microscopy; the samples from thermally driven attachment of carbon structures have been characterized by Nomarski microscopy and scanning electron microscopy. The characterization techniques applied in this thesis work have been introduced in chapter 5 and the sample series information has been listed in chapter 6.

7.1 Cubic Sublimation Growth Process

Cubic sublimation growth process has been performed for reproducing high quality bulk-like 3C-SiC to be used as substrates. The runs have been done in vacuum ambient with 4 degrees off-axis 4H-SiC substrates at growth temperatures of 1850 °C, 1900 °C, 1950 °C, which are corresponding to samples ELS537, ELS539 and ELS542, respectively. Silicon face is the side which is studied.

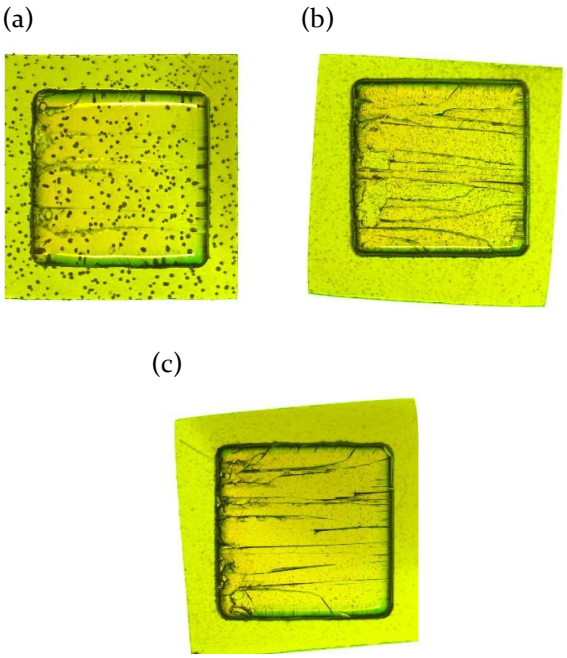

Figure 10: The overview images of (a) ELS537, (b) ELS539 and (c) ELS542.

By comparing the overview images of the three samples, shown in Figure 10, the trend of sample showing more pure yellowish color is observed. The sample of ELS537 has the color of green (4H polytype) and yellow (3C-SiC) mixture; the sample of ELS539 has domains that are yellowish but still some domains remaining greenish; the sample of ELS542 has barely any green part except at edges. While having white light shining through the sample, 3C-SiC is yellow and the 4H-SiC is greenish. Thereby it is easy to see the parts of samples with 3C-SiC and 4H-SiC, or if the sample is fully covered by 3C-SiC (excluding edges).

The trend still remains in all the other samples in the series. This indicates that the higher temperature it is (up till 1950 °C have been performed in the experiment) in CSGP, the more pure and better coverage of 3C-SiC could be produce. The growth rate increases for each temperature increase. Thus the sample grown at highest temperature shows a full 3C-SiC coverage. Thereby the growth temperature of 1950 °C was selected for the study of attachment of carbon allotropes on 3C-SiC.

7.2 Thermal Decomposition of SiC

Thermal decomposition of SiC has been carried out as a pre-study to find conditions for thermally driven attachment of carbon structures. It was applied to reveal at which temperature the surface modification of 4H-SiC on-axis substrates takes place, and at this temperature range it is suitable for the initial study in the thermally driven attachment of carbon structures. Additionally, both Si-rich side and C-rich side of the substrates have been studied regarding thermal decomposition of SiC.

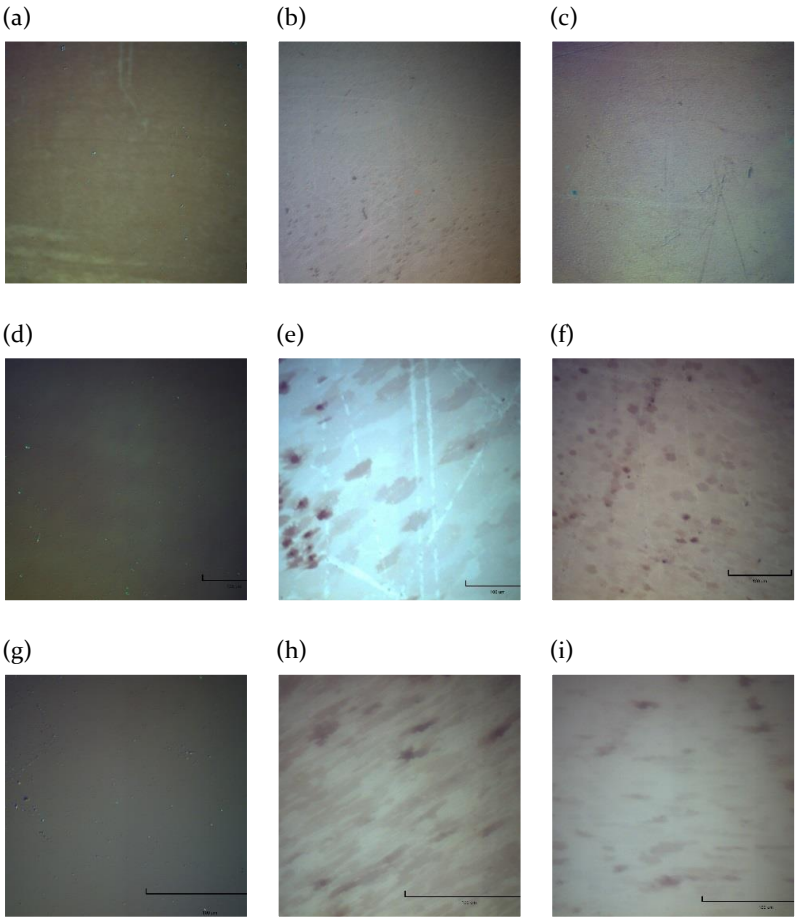

Figure 11: The OM images of thermal decomposition of SiC on Si-rich side. 50X: (a) s602, (b) s604, (c)s606; 200X: (d) s602, (e) s604, (f) s606; 400X: (g) s602, (h) s604, (i) s606

The Nomarski images at different magnifications of thermal decomposition of SiC on the Si-rich side is shown above in Figure 11. The process temperatures of the s602, s604 and s606 are 1800 °C, 1700 °C and 1600 °C, respectively. From the 50X images, no surface features could be observed. This

indicates that the subliming speed has been suppressed by the Ar introduction, so that the macroscopic surfaces are not uneven from the surface reaction which could be is too rapid at a given temperature. A high temperature may cause rapid reaction that is preferential at defects, but no such features are observed even at 1800 °C in our case. Comparing Figure 11 (e) and (f), which are at a higher magnification of 200X, the spots become visible. They seem to be larger in size with increasing process temperature. The spots could be islands that are growing since they differ in size due to the temperature difference. Thermodynamically, the higher temperature it is, the greater energy atoms possess, and hence the larger island sizes could exist. Though no obvious islands could be observed in Figure 11 (d) which shows the sample produced at the highest temperature. Possibly it may have acquired enough energy with the higher temperature so that it grown into continuous island and have full coverage.

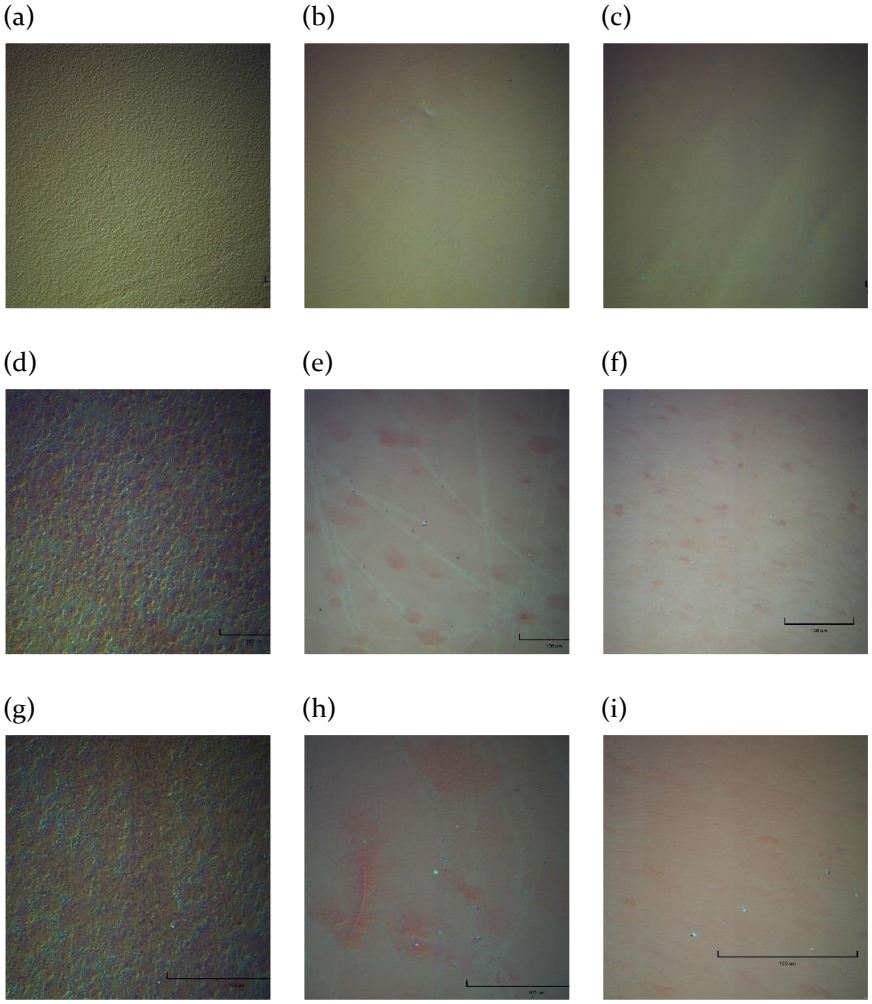

Figure 12: The OM images of thermal decomposition of SiC on C-rich side. 50X: (a) s601, (b) s603, (c)s605; 200X: (d) s601, (e) s603, (f) s605; 400X: (g) s601, (h) s603, (i) s605

The Nomarski images at different magnifications of thermal decomposition of SiC on C-rich side are shown above in Figure 12. The process temperatures of the samples s601, s603and s605 are 1800 ℃, 1700 ℃ and 1600 ℃, respectively. It can be seen that the sample images are generally darker compared to the ones in Figure 11 that were grown on the Si-rich side. This is very likely due to the graphitization that is known to be more severe on the C-rich side than the Si-rich side. Also the sample surfaces of the C-rich side have rougher surface morphologies than the ones of Si-rich side at the same temperature. This agrees with the general fact that C-rich side has lower energy barrier for growth and sublimation than Si-rich side due to its lower surface free energy. Hence, at the limited time and same temperature, C-rich side reacts faster and shows more surface features. On the other hand, islands have grown into larger sizes with higher temperature just as the results from Si-rich side at the highest growth temperature of 1800 ℃. Nevertheless, the rough surface morphologies of s601 could stem from sublimation, and this indicates the temperature of 1800 ℃ gives higher subliming speed on the C-rich side than all the others.

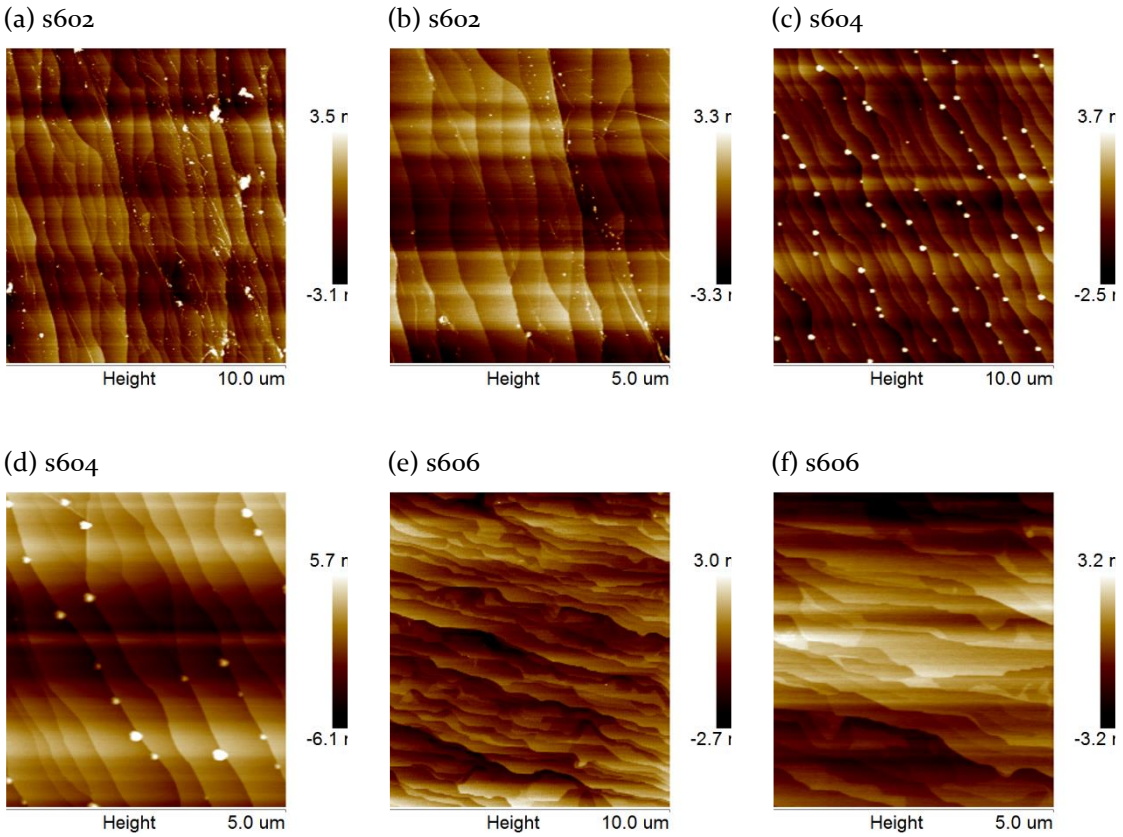

Figure 13: The AFM images of thermal decomposition of SiC on Si-rich side at two scales, 10 μm and 5 μm, respectively. The straight lines from left to right are artefacts from AFM scanning.

Figure 13 shows the AFM images of thermal decomposition of SiC on the Si-rich side at two scales, 10 μm and 5 μm respectively. At the upper right corner of Figure 13 (b), clear stripes that are in the form of cross with lighter color could be observed. And more stripes could be seen on the right side of Figure 13 (a) at lower magnification. The stripes originate while forming a thin film on substrate and gives strain to the substrate. Hence it may indicate that graphene or other films are attempted to form while the sublimation happens, which is close to the epitaxial graphene growth case. In addition, all the images show characteristic features of graphene layers, which agree with the conclusion that there is a film growing. The white dots should be particles that have not been blown away by nitrogen gun, since s606 with extra blowing shows no particle on the images. Also, the step bunching structure of SiC is clearly visible in all cases. This shows that there is surface reaction at all process temperatures.

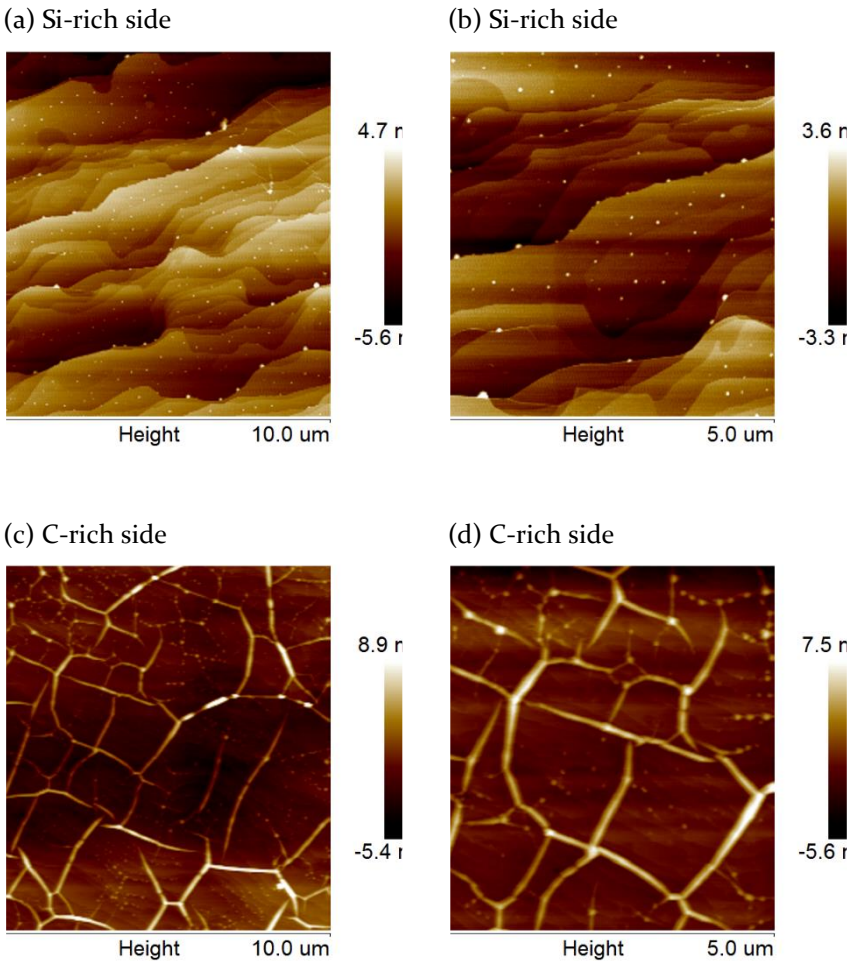

Figure 14: The AFM images of thermal decomposition of SiC on Si- and C-rich side of the same sample s603 at two scales, 10 μm and 5 μm respectively.

Figure 14 shows the AFM images of thermal decomposition of SiC on Si- and C-rich side of the same sample s603 at two scales, 10 μm and 5 μm respectively. In Figure 14 (a) at the upper right corner, the strain stripes are observed again, while in (c) and (d) the stripes could be seen as networks

distributing all over the image. They are characteristic features of graphene or thin graphitic layers on SiC. The comparison of the images agrees with the statement of C-rich side has lower energy barrier than Si-rich side, and that C-rich side reacts faster and shows more surface features at the limited time and same temperature. The cooling of graphene or graphite with SiC causes a thermal stress due to different thermal expansion coefficients of graphene/graphite and SiC. Due to the thickness of graphene /graphite, this causes a pronounced network of strain features.

7.3 Thermally Driven Attachment of Carbon Structures

In the thermally driven attachment of carbon structures study, MWCNTs, fullerene, diamond and graphene nano-sized powder have been distributed on 4H-SiC on-axis substrate and MWCNT on 3C-SiC substrate at 1600 ℃, 1700 ℃ and 1800 ℃. For suppressing the sublimation speed of the powder and the substrate, once the temperature reaches 1000 ℃, 800 mbar of Ar is introduced to the

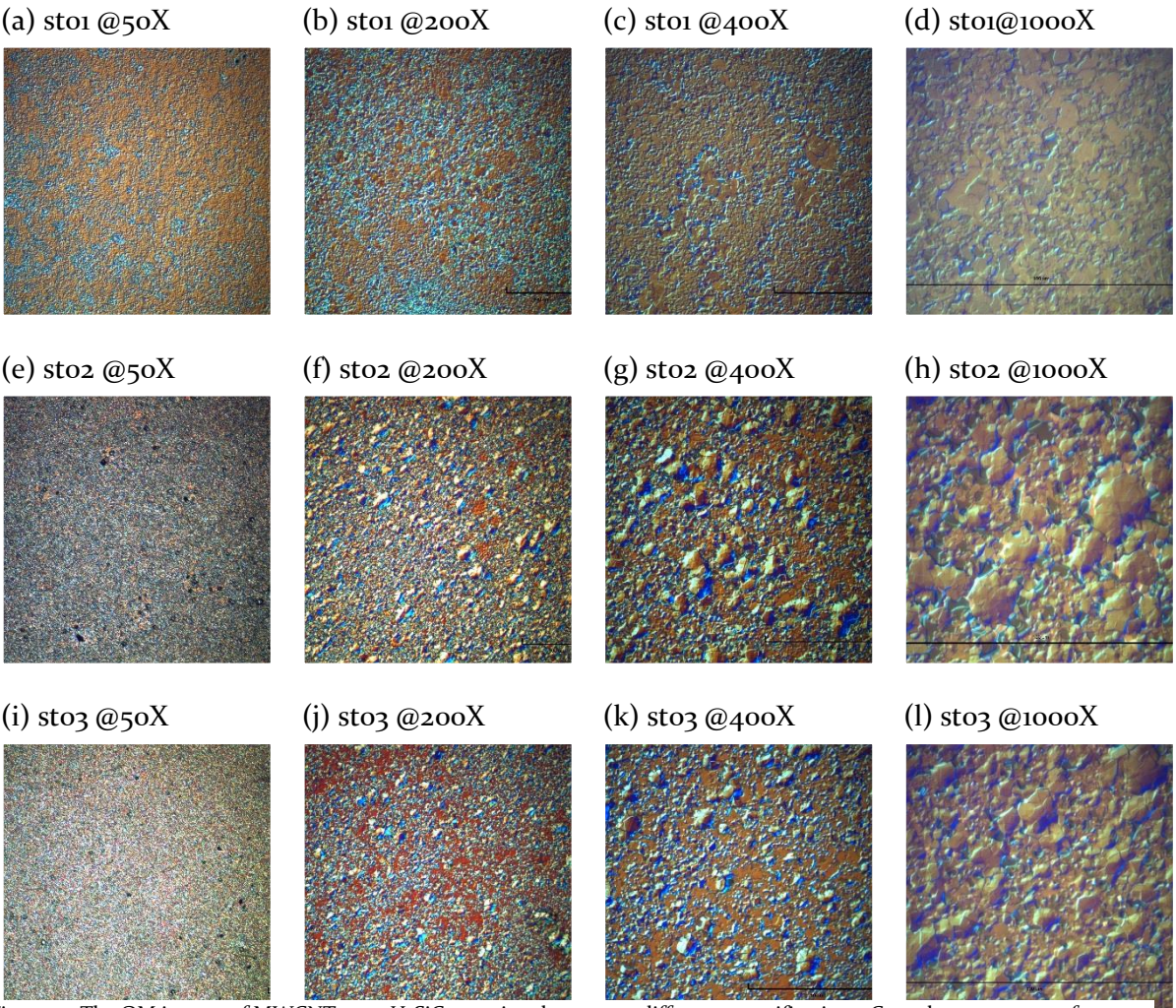

Figure 15: The OM images of MWCNTs on 4H-SiC on-axis substrates at different magnifications. Growth temperatures for st01, st02 and st03 are 1800 ℃, 1700 ℃ and 1600 ℃

chamber. In addition, a reference run with only 4H-SiC on-axis substrate but no powder has been performed. Silicon face is the side which is studied.

Figure 15 shows the Nomarski images of MWCNTs powder on 4H-SiC on-axis substrates at different magnifications. The growth temperatures for st01, st02 and st03 are 1800 °C, 1700 °C and 1600 °C, respectively. Comparing all the images of st02 and st03, it is clear that the higher temperature it is, the larger islands has grown on the sample. This agrees with thermodynamic sense as described earlier. Nevertheless, the sample st01 with the highest growth temperature has the smoothest surface among them. This could be due to the high temperature sublimation and pronounced thermal decomposition. In this scenario the sublimation causes the powder to be sublimed away and no feature remain on the surface more than sublimation features of SiC. From another point of view, it could be indicative of a uniform layer that is present on the surface due to the faster surface kinetics at the highest growth temperature. From still another point of view, the sublimation of SiC could be such that caused the formed islands to be only loosely bound and blown away by nitrogen gun after growth.

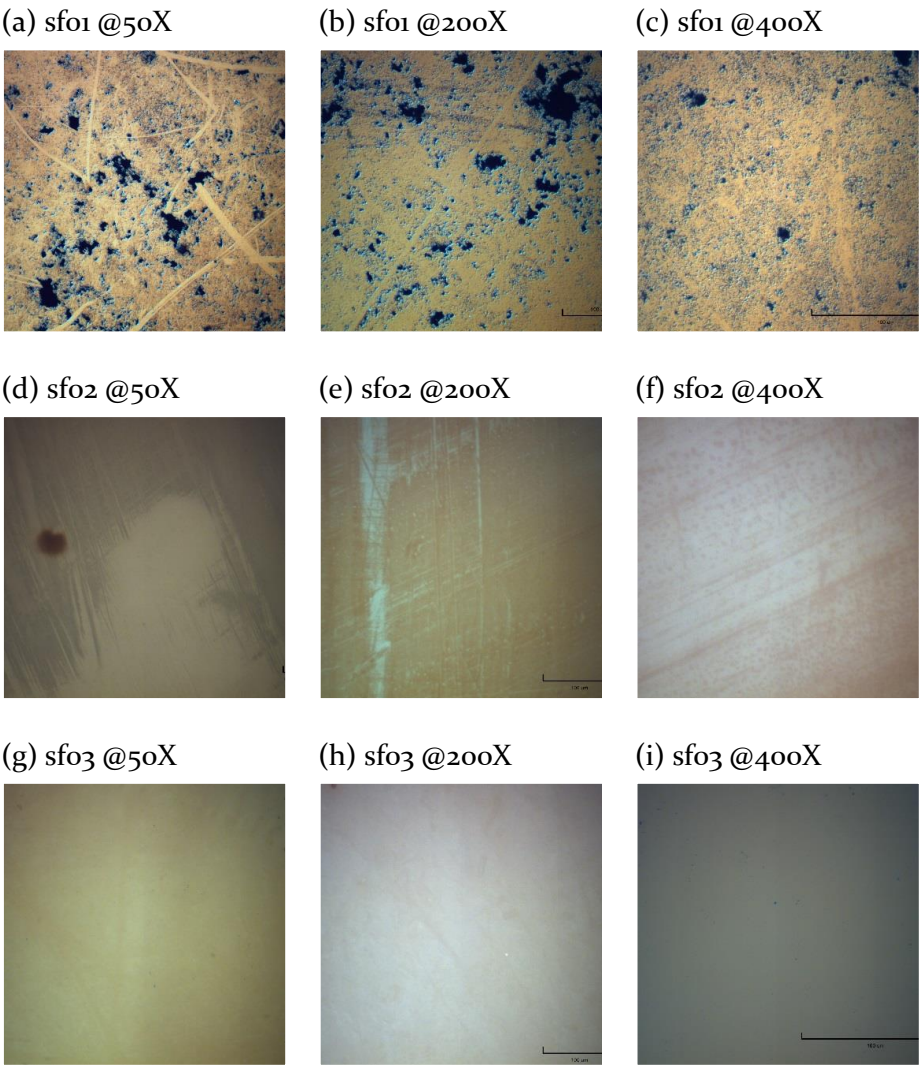

Figure 16: The OM images of fullerene on 4H-SiC on-axis substrates at different magnifications. Growth temperatures for sfo1, sfo2 and sfo3 are 1800 ℃, 1700 ℃ and 1600 ℃

Figure 16 shows the Nomarski images of fullerene powder on 4H-SiC on-axis substrates at different magnifications. The growth temperatures for sf01, sf02 and sf03 are 1800 °C, 1700 °C and 1600 °C, respectively. From the images of sf02 and sf03, no surface features could be seen. One could possibly expect such result since a fullerene is an enormous structure comparing to the others, and it is spherical which leads to less number of bonds and edges that could attach. Nevertheless, it is observed that sf01, with the highest growth temperature, has some surface features. This should be thermal decomposition and sublimation of atoms, leaving the surface with rough morphology. In addition, even there had been fullerene attached onto these substrates, the islands could be detached and blown away when blowing the surface by the nitrogen gun.

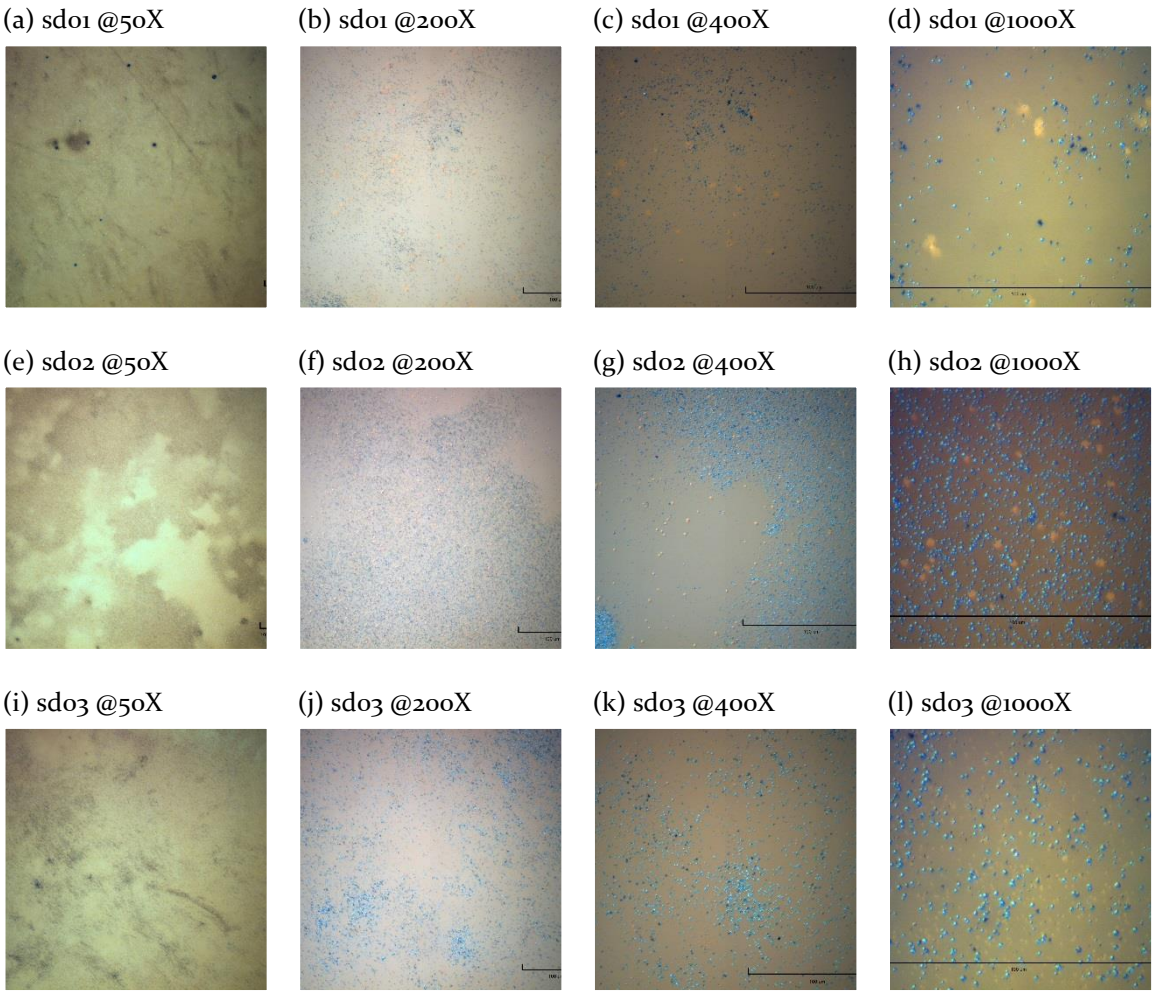

Figure 17: The OM images of diamond on 4H-SiC on-axis substrates at different magnifications. Growth temperatures for sd01, sd02 and sd03 are 1800 °C, 1700 °C and 1600 °C.

Figure 17 shows the Nomarski images of diamond powder on 4H-SiC on-axis substrates at different magnifications. The growth temperatures for sd01, sd02 and sd03 are 1800 ℃, 1700 ℃ and 1600 ℃, respectively. In all the images, bright particles could be observed. The assumption is that the particles are diamond particles clustering since they have not been observed in other sample and they are non-symmetrically distributed. Diamond is a very stable structure, and diamond nano-sized powder on the surface could be present but not change or expand the diamond structure or grow in similar way like MWCNTs which could be supported by remaining carbon from the sublimation of the SiC surface.

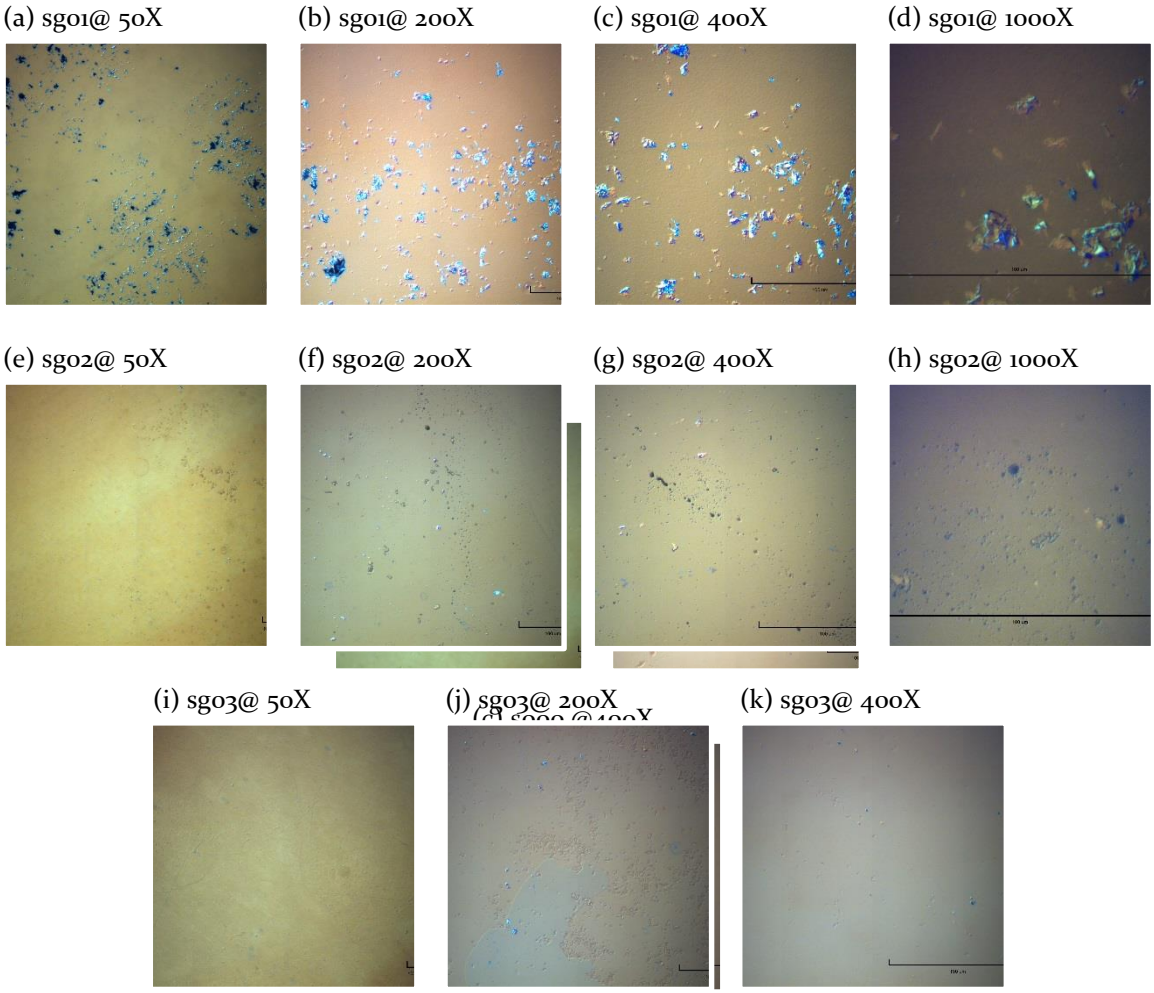

Figure 19: The OM images of 4H-SiC on-axis bare substrate at different magnifications.

Figure 18: The OM images of graphene on 4H-SiC on-axis substrates at different magnifications. Growth temperatures for sg01, sg02 and sg03 are 1800 ℃, 1700 ℃ and 1600 ℃

Figure 18 shows the Nomarski images of graphene powder on 4H-SiC on-axis substrates at different magnifications. The growth temperatures for sg01, sg02 and sg03 are 1800 ℃, 1700 ℃ and 1600 ℃, respectively. In the images of sg01, bright islands could be observed clearly, large in size and higher amount. They could also be seen but in less amount and smaller in size in sg02 and sg03

images. The speculation is that the bright islands are SiC islands forming from silicon rich regions since graphene powder is light in weight, very small and attaching together as flakes, or react with the Si and C species that form at the sublimation of SiC. In SiC sublimation, Si forms first and Si_2C and SiC_2 forms next due to the vapor pressures of the species. Thus it is reasonable that Si could react with the small graphene powder flakes and form SiC. The islands growing trend is also matching the thermodynamic statement from previous discussions.

Figure 19 shows the Nomarski images of 4H-SiC on-axis bare substrate having process temperature at 1600 ℃ with different magnifications. This serves as reference run to ensure the conditions of the growth system are reliable by observing the surface modification of 4H-SiC on-axis substrate after the thermally driven attachment of carbon structures on 4H-SiC on-axis substrate. The images show that no contaminations nor unexpected surface features, and hence the thermally driven attachment of carbon structures on 3C-SiC could be performed at similar conditions since the series were performed at different times.

(a) ELS525 (b) ELS522

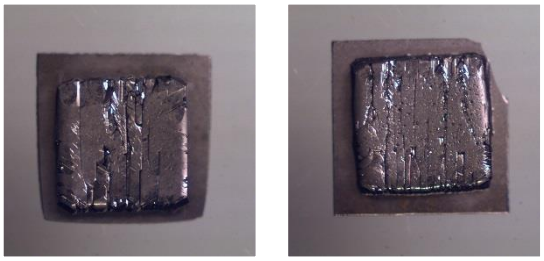

(c) ELS526

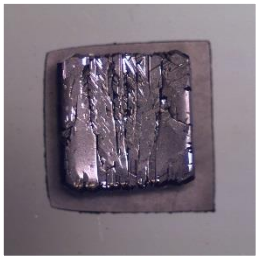

Figure 20: The overview images of MWCNTs on 3C-SiC at different growth temperatures.

Figure 20 shows the overview images of MWCNTs on 3C-SiC at different temperatures. The growth temperatures of ELS525, ELS522 and ELS526 are 1800 ℃, 1700 ℃ and 1600 ℃, respectively. The surface roughness of the samples are due to the as-grown character of the 3C-SiC. The color transforming from transparent yellow to non-transparent gray indicates that there is another film grown on the substrate. The 3C-SiC substrate original images have been shown in Figure 10.

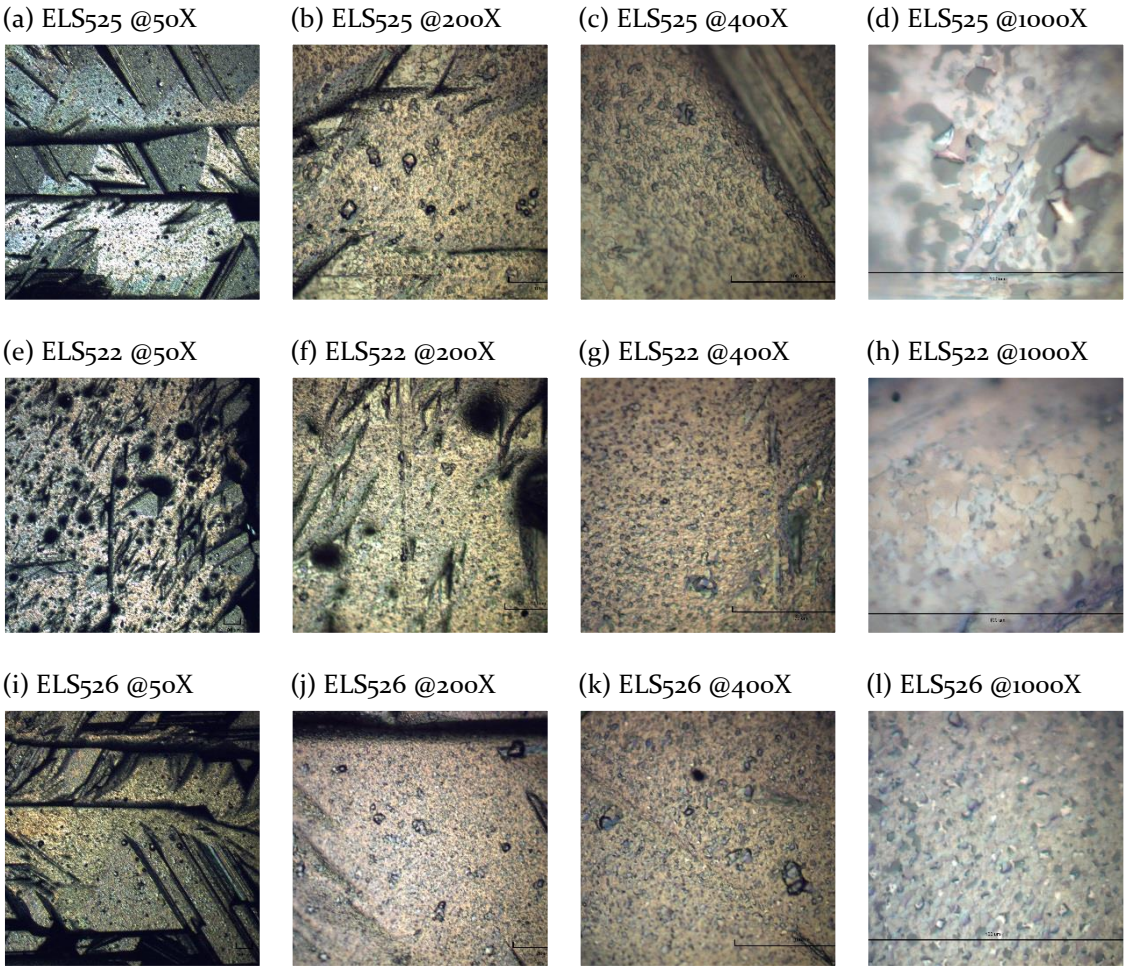

Figure 21: The OM images of MWCNTs on 3C-SiC substrates at different magnifications. Growth temperatures of ELS525, ELS522 and ELS526 are 1800 °C, 1700 °C and 1600 °C

Figure 21 shows the Nomarski images of MWCNTs on 3C-SiC substrates at different magnifications. The growth temperatures of ELS525, ELS522 and ELS526 are 1800 °C, 1700 °C and 1600 °C, respectively. Due to the surface roughness from as-grown 3C-SiC and different polytype of substrates, the images differ greatly from the ones of 4H-SiC on-axis substrates in Figure 15. Nevertheless, in all cases islands are observed and this shows that there is thermally driven attachment also in this case. Also, the islands which could be observed are clearer at higher magnifications in all three samples, and thus the islands follow the trend of larger sized islands with higher growth temperatures.

(a) st01 @120μm (b) st01 @40μm (c) st01 @20μm

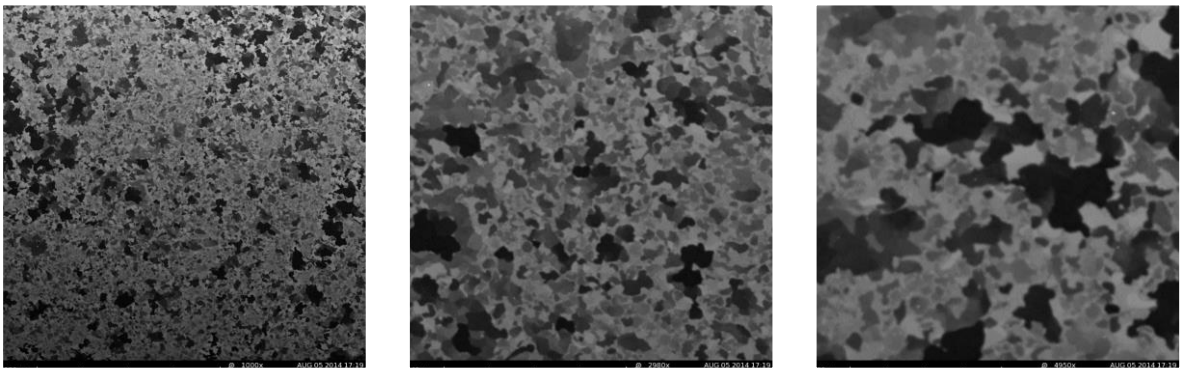

(d) st02 @110μm (e) st02 @40μm (f) st02 @20μm

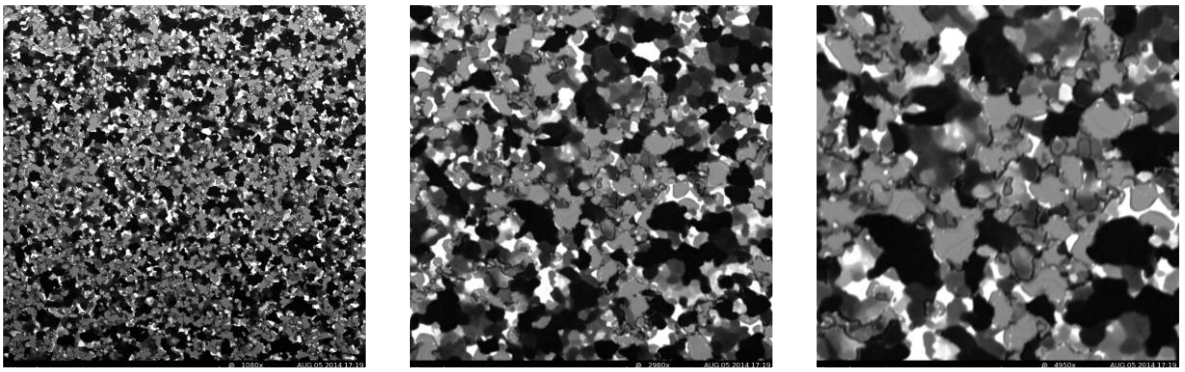

(g) st03 @110μm (h) st03 @40μm (i) st03 @20μm

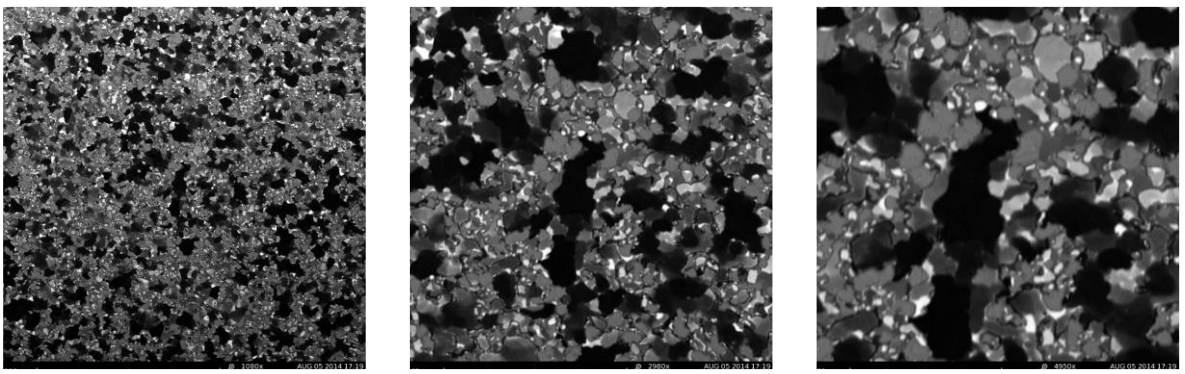

Figure 22: The SEM images of MWCNTs on 4H-SiC on-axis substrates at different magnifications.

Figure 22 displays the SEM images of MWCNTs on 4H-SiC on-axis substrates at different magnifications. From Figure 22 (a), (b) and (c), the speculations of the high temperature sublimation and thermal decomposition are in agreement. This is due to the residual islands that could be seen, and they have the same shape as the islands in the two other samples. Hence with the more uniform surface, the islands are detached and blown away when blown by the nitrogen gun for st01. In addition, with the larger depth of focus of SEM images, it is easier to compare the size of the islands

when more islands are in focus. Here, we can see clearly that there is the trend of islands growing larger when the growth temperature is higher. The relationship between island sizes and temperature could also indicate that the thermally driven attachment of carbon structure is effective.

Figure 23 shows the SEM images for comparison of MWCNTs on 3C-SiC and on 4H-SiC on-axis

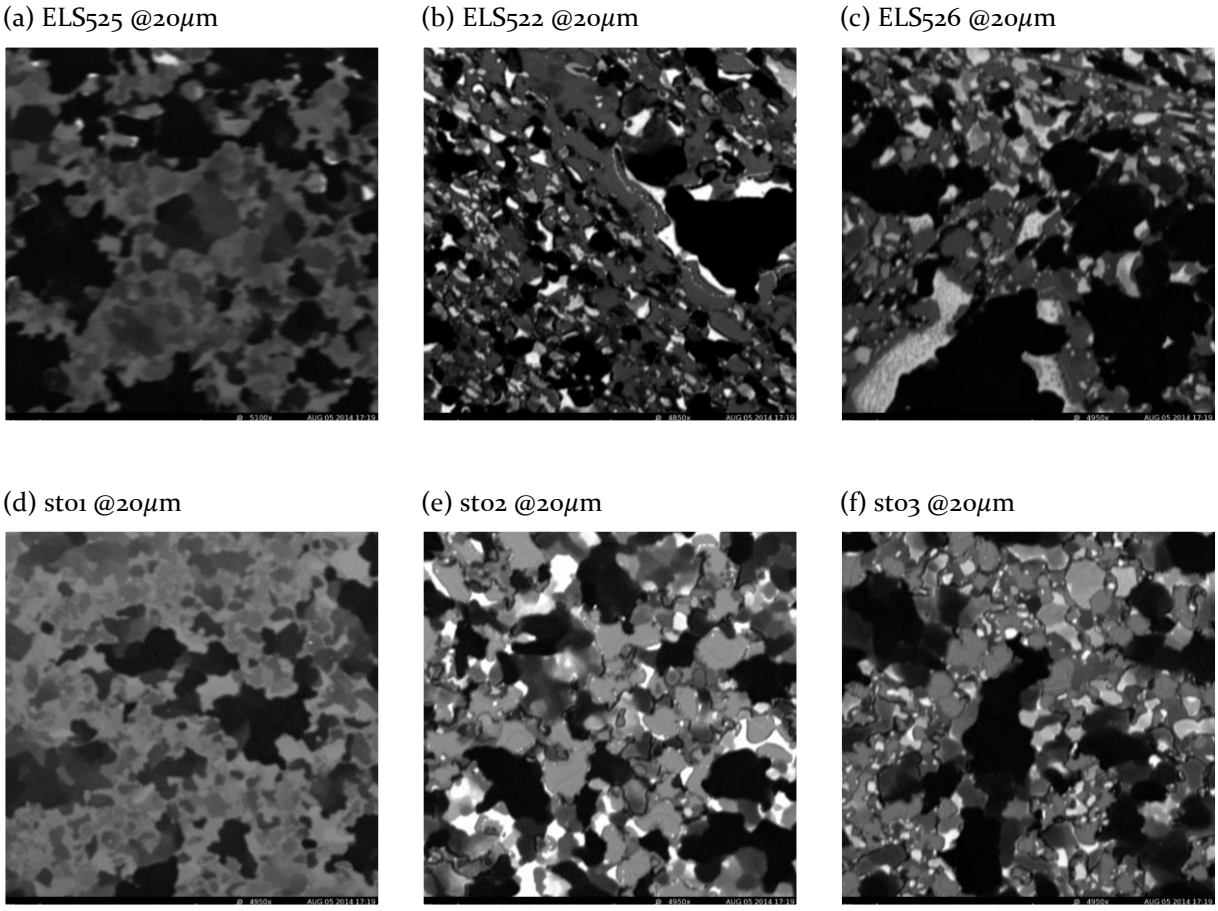

Figure 23: The comparison of SEM images from MWCNTs on 3C-SiC and on 4H-SiC on-axis substrates.

substrates. With the same size of areas chosen for the images, the islands sizes of MWCNTs on 3C-SiC and 4H-SiC on-axis substrates at the same temperature could be compared. Neglecting the image from sto1 due to its probability of having detached islands, Figure 23 (b) and (c) can be compared with (e) and (f) respectively. It can be seen that the average islands sizes of samples from 4H-SiC on-axis substrates are larger than the ones from 3C-SiC substrates. This could also be explained as previously, that the different conditions of roughness and polytypes the substrates cause the growth to be effective in different ways. It was also observed in graphene growth on 3C-SiC, 6H-SiC, and 4H-SiC, that there is a slight difference in growth of graphene on the different polytypes [4]. In our case, the images with 3C-SiC substrates have unpolished and fairly rough surfaces due to the as-grown surface used, and hence there are difficulties to find large flat terrace which give rise to the uneven

or tilted area in the images. In any case, there is clearly attachment on both 3C-SiC and 4H-SiC, while some differences between polytypes could be expected but not to any substantial extent.

8. CONCLUSIONS

The 3C-SiC growth on 4 degrees off-axis 4H-SiC substrate has been performed with the same standard of setup and the same controlled growing parameters, with samples series ranging from ELS533 till ELS545 at growth temperatures of 1850 ℃, 1900 ℃ and 1950 ℃ all within vacuum level of $10^{-5}\ mbar$. The purpose of reproducing good quality of bulk 3C-SiC has been achieved with higher growth temperature, which is 1950 ℃ in this thesis work, and fabrication of 3C-SiC with full coverage of 3C-SiC that could be used as substrates in the attachment study.

Thermal decomposition of SiC has been performed on 4H-SiC on-axis substrate which would be applied in a study of thermally driven attachment of carbon structures. In macroscopic observation from the Nomarski images, no obvious surface features could be seen, which indicates that the introduction of 800 mbar Ar into chamber temperature reaches 1000 ℃ during the heating successfully suppressed the sublimation speed of the substrate surface atoms. Nevertheless, since no obvious surface features could be seen, the strain stripes shown in could prove that certain film has been forming or attempt to form at 1800 ℃. And though no stripes has been shown in other images from Si-rich sides, it could be seen that islands have been forming and growing influenced by the process temperature. The surface morphology modification exists in all samples, which gives the attaching opportunities. Hence, the thermally driven attachment of carbon structures could be performed with these 4H-SiC on-axis substrates at 1800 ℃, 1700 ℃ and 1600 ℃ as in thermal decomposition. Furthermore, it could be seen that the sample surfaces of C-rich side have rougher surface morphologies than the ones of Si-rich side at the same process time and temperature. This agrees with the general fact that C-rich side has lower energy barrier than Si-rich side, and hence at the same limited time and temperature, C-rich side reacts faster and shows more surface features.

The thermally driven attachment of carbon structures of MWCNTs, fullerene, diamond and graphene nano-sized powder distributed on 4H-SiC on-axis substrate and MWCNT on 3C-SiC substrate at 1600 ℃, 1700 ℃ and 1800 ℃ have been implemented. For the first time, there is initial understanding the temperature effect on the attachment and the difference using 4H-SiC on-axis substrate or 3C-SiC substrate. Also for suppressing the sublimation speed of the powder and the substrate, once the temperature reaches 1000 ℃, 800 mbar of Ar is introduced to the chamber as a crucial step. In general, the trend is that whenever there had been islands growing on the sample surfaces, they all followed the thermodynamic behavior: the higher temperature it is, the greater energy the atoms possess, and hence the larger island sizes could exist. For MWCNTs on 4H-SiC on-axis substrates, the highest growth temperature may cause a high temperature sublimation and thermal decomposition, leading to more uniform surface, and hence any islands that had grown on the surface are detached and blown away by the nitrogen gun.

For fullerene on 4H-SiC on-axis substrates, no surface features could be seen. Since fullerene is a larger structure comparing to the others, and it is spherical, there could be poor attachment to few bonds and small attachment area. At the highest growth temperature, has some surface features could be from thermal decomposition and sublimation of atoms. For diamond on 4H-SiC on-axis substrates, bright particles could be observed in all samples. The particles could be diamond particles clustering since they have not been observed in other sample and they are non-symmetrically distributed. For graphene on 4H-SiC on-axis substrates, bright islands at different sizes could be observed in all samples. The islands are bright, which excluded the assumption of graphite, graphene

or other products. They could be SiC islands forming from silicon sublimation that reacts with the light graphene flakes. In addition, due to the low growth temperature, the possibility is that they are 3C-SiC islands.

Experiments of MWCNTs on 3C-SiC substrates have been performed using MWCNTs since they showed clear features on 4H-SiC on-axis substrates. Average islands sizes of samples from 4H-SiC on-axis substrates are larger than the ones from 3C-SiC substrates. This could be due to the different conditions of surface roughness and polytypes of the substrates.

9. FUTURE WORK

For confirming the results and conclusions acquired in this thesis work, the future researchers should have trials to reproduce the experiments and results. In addition, more characterization techniques could be performed on the samples. For instance, X-ray photoelectron spectroscopy (XPS) could be performed on the 3C-SiC film for acquiring the elemental composition, and that transmission electron microscopy (TEM) could be performed on 3C-SiC for identifying the defects, etc.

In this thesis work, the 3C-SiC as-grown samples are not polished and have surface roughness. They could be polished carefully and try to have the attachment on smooth surfaces with even more variety of carbon allotropes. Furthermore, the 4H-SiC on-axis substrate used in the thermal decomposition of SiC and thermally driven attachment of carbon structures could be replaced by 4 degrees off-axis 4H-SiC substrate. Since the 3C-SiC has been grown on 4 degrees off-axis 4H-SiC substrate, the replacement assures the comparison of the results of thermally driven attachment of carbon structures is with more common conditions.

Eventually, the design could be modified for wide diversity of applications, such as bio-usage, electric devices, electrode material, etc.

10. REFERENCES

[1] J. J. R. Casady, "Status of silicon carbide (SiC) as a wide-bandgap semiconductor for high-temperature applications: A review," *Solid-State Electronics,* vol. 39, no. 10, pp. p.1409-1422, 1996.

[2] T. Y. K. M. M. I. T. H. Masashi Kato, "Epitaxial p-type SiC as a self-driven photocathode for water splitting," *International Journal of Hydrogen Energy,* 2014.

[3] D. W. C. J.-B. B. a. W. L. Liming Dai, "Carbon Nanomaterials for Advanced Energy Conversion and Storage," *Carbon Nanomaterials,* pp. 1130-1166, 2011.

[4] R. V. T. I. A. Z. M. S. R. Y. G. Reza Yazdi, "Growth of large area monolayer graphene on 3C-SiC and a comparison with other SiC polytypes," *Carbon,* 2013.

[5] E. Janzen, O. Kordina, A. Henry, W. Chen, N. Son, B. Monemar, E. Sorman, P. Bergman, C. Harris, R. Yakimova, M. Tuominen, A. Konstantinov, C. Hallin and C. Hemmingsson, "SiC - a semiconductor for high-power, high-temperature and high-frequency devices," *Physica Scripta,* vol. T54, pp. 283-290, 1994.

[6] A. S. Cheng, "Study of 3C and 6H SiC Polytype Stability in Sublimation Epitaxial Growth Using on-axis Substrates," Linköping Univ., Linköping, 2010.

[7] P. H. Chen, "Stability of Bulk Cubic Silicon Carbide (3C-SiC) on Off Oriented Hexagonal Silicon (4H-SiC) Substrate," Linköping Univ., Linköping, 2013.

[8] G. S. B. a. A. Zangwill, "Morphological instability of a terrace edge during step-flow growth," *Physical Review B,* vol. 41, 1990.

[9] A. Fissel, "Thermodynamic considerations of the epitaxial growth of SiC polytypes," *Journal of Crystal Growth,* vol. 212, pp. 438-450, 2000.

[10] E. S. S. N. Mokhov, "Structural Perfection of Silicon Carbide Crystals Grown on Profiled Seeds by Sublimation Method," *Materials Science Forum,* Vols. 740-742, pp. 60-64, 2013.

[11] P. G. P. A. J. Neudeck, "Performance Limiting Micropipe Defects in Silicon Carbide Wafers," *Source of the DocumentIEEE Electron Device Letters,* vol. 15, pp. 63-65, 1994.

[12] C. H. S. S. K. Z. H. N. H. T. M. U. T. Zhu, "Influence of Solution Flow on Step Bunching in Solution Growth of SiC Crystals," *Crystal Growth and Design,* vol. 13, pp. 3691-3696, 2013.

[13] N. K. K. N. A. T. K. Shirahata, "Thermal Stability of Stacking Faults in Beta-SiC," *Nippon Seramikkusu Kyokai Gakujutsu Ronbunshi/Journal of the Ceramic Society of Japan,* Vols. 161-163, pp. 623-626, 1999.

[14] B. L. J. J. T. G. a. G. A. R. H. S. Kong, "An examination of double positioning boundaries and interface misfit in beta-SiC films on alpha-SiC substrates," *Journal of Applied Physics,* vol. 63, pp. 2645-2650, 1988.

[15] P. Wothers, "The Modern Alchemist: Allotropes of Carbon," 2012. [Online]. Available: http://www.richannel.org/.

[16] E. R. M. R. A. V. Y. Mokhov, "SiC growth in tantalum containers by sublimation sandwich method," *Journal of Crystal Growth,* vol. 181, pp. 254-258, 1997.

[17] Y. Leng, in *Materials Characterization: Introduction to Microscopic and Spectroscopic Methods, 2nd Edition*, Wiley-VCH, 2013, pp. 35-37.

[18] P. R. I. r. i. Boehlke, "Scanning electron microscopy," *IIT research institute,* 1968.

[19] D. H. a. D. Bacon, Introduction to Dislocations, 3rd edition, University of Liverpool, 1984.

[20] M.-H. W. S. N. M. Sergei N. Magonov, Surface Analysis with STM and AFM: Experimental and Theoretical Aspects of Image Analysis, Wiley-VCH, 1996.

[21] G. D. W. G. L. J. Hoffmann, "Micro-Raman and tip-enhanced Raman spectroscopy of carbon allotropes," *Macromolecular Symposia,* vol. 265, pp. 1-11, 2008.